NOVEL HYDROGEN COMPOUNDS FROM A POTASSIUM CARBONATE ELECTROLYTIC CELL

RANDELL L. MILLS* *BlackLight Power*
493 Old Trenton Road, Cranbury, New Jersey 08512

Novel compounds containing hydrogen in new hydride and polymeric states that demonstrate novel hydrogen chemistry have been isolated following the electrolysis of a K_2CO_3 electrolyte with the production of excess energy. Inorganic hydride clusters $K[KH\ KHCO_3]_n^+$ and hydrogen polymer ions such as OH_{23}^+ and H_{16}^- were identified by time-of-flight secondary ion mass spectroscopy. The presence of compounds containing new states of hydrogen was confirmed by X-ray photoelectron spectroscopy, X-ray diffraction, Fourier transform infrared spectroscopy, Raman spectroscopy, and proton nuclear magnetic resonance spectroscopy.

I. INTRODUCTION

A hydride ion comprises two indistinguishable electrons bound to a proton. Alkali and alkaline earth hydrides react violently with water to release hydrogen gas that subsequently ignites because of the exothermic reaction with water. Typically, metal hydrides decompose upon heating at a temperature well below the melting point of the parent metal. These saline hydrides, so called because of their saltlike or ionic character, are the monohydrides of the alkali metals and the dihydrides of the alkaline-earth metals.

A novel hydride ion having extraordinary chemical properties, given by Mills,[1] is predicted to form by the reaction of an electron with a hydrino [Eq. (2)], a hydrogen atom having a binding energy given by

$$Binding\ Energy = \frac{13.6\ eV}{\left(\dfrac{1}{p}\right)^2}, \qquad (1)$$

where p is an integer >1, designated as $H[a_H/p]$ where a_H is the radius of the hydrogen atom. The resulting hydride ion is referred to as a hydrino hydride ion, designated as $H^-(1/p)$:

$$H\left[\frac{a_H}{p}\right] + e^- \rightarrow H^-(1/p) . \qquad (2)$$
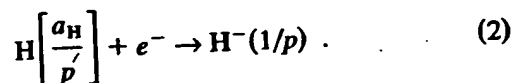
The hydrino hydride ion is distinguished from an ordinary hydride ion having a binding energy of 0.8 eV. The latter is hereafter referred to as "ordinary hydride ion." The hydrino hydride ion is predicted[1] to comprise a hydrogen nucleus and two indistinguishable electrons at a binding energy according to the following formula:

$$Binding\ Energy = \frac{\hbar^2\sqrt{s(s+1)}}{8\mu_e a_0^2 \left[\dfrac{1+\sqrt{s(s+1)}}{p}\right]^2}$$

$$- \frac{\pi\mu_0 e^2 \hbar^2}{m_e^2 a_0^3}$$

$$\times \left(1 + \frac{2^2}{\left[\dfrac{1+\sqrt{s(s+1)}}{p}\right]^3}\right), \qquad (3)$$

where

p = integer >1

$s = \frac{1}{2}$

π = pi

$\hbar$ = Planck's constant bar

μ_0 = permeability of vacuum

m_e = mass of the electron

*E-mail: rmills@blacklightpower.com

μ_e = reduced electron mass

a_0 = Bohr radius

e = elementary charge.

The ionic radius is

$$r_1 = \frac{a_0}{p}(1 + \sqrt{s(s+1)}), \quad s = \frac{1}{2} \ . \tag{4}$$
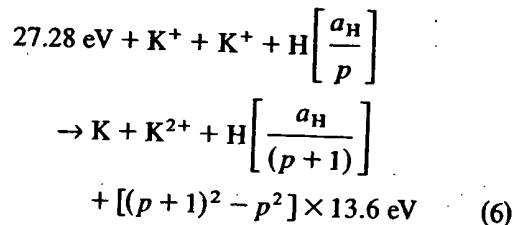
From Eq. (4), the radius of the hydrino hydride ion $H^-(1/p)$, p = integer, is $1/p$ that of the ordinary hydride ion, $H^-(1/1)$. The binding energies and radii of the first 16 hydride ions, $H^-(n = 1/p)$ as a function of p, where p is an integer, are shown in Table I.

Hydrinos are predicted to form by reacting an ordinary hydrogen atom with a catalyst having a net enthalpy of reaction of about
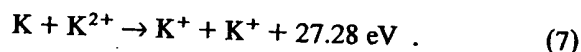
$$m \cdot 27.21 \text{ eV} \ , \tag{5}$$

where m is an integer.[1] This catalysis releases energy from the hydrogen atom with a commensurate decrease in size of the hydrogen atom, $r_n = na_H$. For example, the catalysis of $H(n = 1)$ to $H(n = \frac{1}{2})$ releases 40.8 eV, and the hydrogen radius decreases from a_H to $\frac{1}{2}a_H$. One such catalytic system involves potassium. The second ionization energy of potassium is 31.63 eV, and K^+ releases
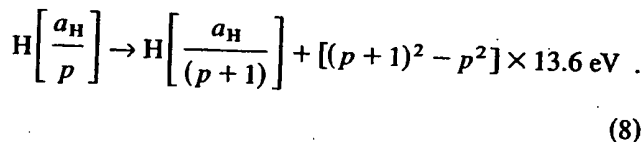
TABLE I

The Representative Radius and Binding Energy of the Hydrino Hydride Ion $H^-(n = 1/p)$ as a Function of p

Hydride Ion	$r_1 \ (a_0)^a$	Binding Energy (eV)^b	Wavelength (nm)
$H^-(n = \frac{1}{1})$	1.8660	0.7540	1644
$H^-(n = \frac{1}{2})$	0.9330	3.047	407
$H^-(n = \frac{1}{3})$	0.6220	6.610	188
$H^-(n = \frac{1}{4})$	0.4665	11.23	110
$H^-(n = \frac{1}{5})$	0.3732	16.70	74.2
$H^-(n = \frac{1}{6})$	0.3110	22.81	54.4
$H^-(n = \frac{1}{7})$	0.2666	29.34	42.3
$H^-(n = \frac{1}{8})$	0.2333	36.08	34.4
$H^-(n = \frac{1}{9})$	0.2073	42.83	28.9
$H^-(n = \frac{1}{10})$	0.1866	49.37	25.1
$H^-(n = \frac{1}{11})$	0.1696	55.49	22.3
$H^-(n = \frac{1}{12})$	0.1555	60.97	20.3
$H^-(n = \frac{1}{13})$	0.1435	65.62	18.9
$H^-(n = \frac{1}{14})$	0.1333	69.21	17.9
$H^-(n = \frac{1}{15})$	0.1244	71.53	17.3
$H^-(n = \frac{1}{16})$	0.1166	72.38	17.1

^{a}Equation (4).
^{b}Equation (3).

4.34 eV when it is reduced to K. The combination of reactions K^+ to K^{2+} and K^+ to K, then, has a net enthalpy of reaction of 27.28 eV, which is equivalent to $m = 1$ in Eq. (5):

$$27.28 \text{ eV} + K^+ + K^+ + H\left[\frac{a_H}{p}\right]$$
$$\rightarrow K + K^{2+} + H\left[\frac{a_H}{(p+1)}\right]$$
$$+ [(p+1)^2 - p^2] \times 13.6 \text{ eV} \tag{6}$$

and

$$K + K^{2+} \rightarrow K^+ + K^+ + 27.28 \text{ eV} \ . \tag{7}$$

The overall reaction is

$$H\left[\frac{a_H}{p}\right] \rightarrow H\left[\frac{a_H}{(p+1)}\right] + [(p+1)^2 - p^2] \times 13.6 \text{ eV} \ . \tag{8}$$

The energy given off during catalysis is much greater than the energy lost to the catalyst. The energy released is large as compared to conventional chemical reactions. For example, when hydrogen and oxygen gases undergo combustion to form water,

$$H_2(g) + \frac{1}{2}O_2(g) \rightarrow H_2O(l) \ , \tag{9}$$
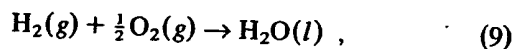
the known enthalpy of formation of water is $\Delta H_f = -286$ kJ/mol or 1.48 eV per hydrogen atom. By contrast, each $(n = 1)$ ordinary hydrogen atom undergoing catalysis releases a net of 40.8 eV. Moreover, further catalytic transitions may occur: $n = \frac{1}{2} \rightarrow \frac{1}{3}, \frac{1}{3} \rightarrow \frac{1}{4}, \frac{1}{4} \rightarrow \frac{1}{5}$, and so on. Once catalysis begins, hydrinos autocatalyze further in a process called disproportionation.[1] This mechanism is similar to that of an inorganic ion catalysis. But, hydrino catalysis should have a higher reaction rate than that of the inorganic ion catalyst because of the better match of the enthalpy to $m \times 27.2$ eV.

Hydrino hydride ions may react with cations to produce compounds such as alkali and alkaline earth hydrides. A representative compound has the formula $MH_mM'X$, wherein m is an integer, M and M' are each an alkali or alkaline earth cation, X is a singly or doubly negative charged anion, and the hydrogen content H_m of the compound comprises at least one hydrino hydride ion. For example, an inorganic hydride compound having the formula $KH \ KHCO_3$ was isolated from an aqueous K_2CO_3 electrolytic cell reactor. Inorganic hydride clusters $K[KH \ KHCO_3]_n^+$ were identified by time-of-flight secondary ion mass spectroscopy (TOF-SIMS). A hydride ion with a binding energy of 22.8 eV has been observed by X-ray photoelectron spectroscopy (XPS) and has upfield shifted solid-state magic-angle spinning proton nuclear magnetic resonance (^{1}H MAS NMR) peaks. Moreover, a polymeric structure is indicated by Fourier

transform infrared (FTIR) spectroscopy. Additional high binding energy hydride ions of other novel alkali and alkaline earth hydrides were observed by XPS. In addition, polyhydrogen compounds may form because hydrino atoms and hydrino hydride ions have orbitals other than the s orbital, which may participate in bonding. Hydrogen polymer ions such as OH_{23}^+ and H_{16}^- were identified by TOF-SIMS.

The discovery of novel hydrogen species such as hydride ions with high binding energies has implications for a new field of hydrogen chemistry. These novel compositions of matter and associated technologies may have far-reaching applications in many industries, including chemical, electronics, computer, military, energy, and aerospace, in the form of products such as batteries, propellants, solid fuels, munitions, surface coatings, structural materials, and chemical processes.

II. EXPERIMENTAL

II.A. Electrolytic Cells

Thermacore (Lancaster, Pennsylvania) operated a K_2CO_3 electrolytic cell consisting of a nickel wire cathode and platinized titanium anodes described by Mills et al.[2] and herein referred to as the Thermacore electrolytic cell. This cell had produced an enthalpy of formation of increased binding energy hydrogen compounds of 1.6×10^9 J that exceeded the total input enthalpy given by the product of the electrolysis voltage and current over time by a factor >8. Briefly, the cell vessel comprised a 10-gal (33- X 15-in.) Nalgene tank. An outer cathode consisted of 5000 m of 0.5-mm-diam clean, cold drawn nickel wire[a] wound on a polyethylene cylindrical support. A central cathode comprised 5000 m of the nickel wire wound in a toroidal shape. The central cathode was inserted into a cylindrical, perforated polyethylene container that was placed inside the outer cathode with an anode array between the central and outer cathodes. The anode comprised an array of 15 platinized titanium anodes.[b] Before assembly, the anode array was cleaned in 3 M HCl for 5 min and rinsed with distilled water. The cathode was cleaned by placing it in a tank of 0.57 M $K_2CO_3/3\%$ H_2O_2 for 6 h and then by rinsing it with distilled water. The anode was placed in the support between the central and outer cathodes, and the electrode assembly was placed in the tank containing electrolyte. The electrolyte solution comprised 28 ℓ of 0.57 M K_2CO_3 (Alfa K_2CO_3 99%).

---

[a]NI 200 0.0197 in., HTN36NOAG1, from A-1 Wire Tech, Inc., 840-39th Avenue, Rockford, Illinois 61109.
[b]Ten of the anodes were Engelhard Pt/Ti mesh, 1.6 X 8 in. with one $\frac{3}{4}$ X 7-in. stem attached to the 1.6-in. side plated with 100 U series 3000; five of the anodes were Engelhard 1-in.-diam X 8-in.-long titanium tubes with one $\frac{3}{4}$ X 7-in. stem affixed to the interior of one end and plated with 100 U Pt series 3000.

Electrolysis was performed at 20-A constant current with a constant current ($\pm 0.02\%$) power supply.

A cell that produced 6.3×10^8 J of enthalpy of formation of increased binding energy hydrogen compounds was operated by BlackLight Power (Malvern, Pennsylvania), herein referred to as the BLP electrolytic cell. The cell description is also given in Ref. 2 except that it lacked the additional central cathode.

Idaho National Engineering Laboratory (INEL) operated a cell,[3] herein referred to as the INEL electrolytic cell, identical to the Thermacore electrolytic cell except that it lacked the central cathode and that the cell was wrapped in a 1-in. layer of urethane foam insulation about the cylindrical surface. The cell was operated in a pulsed power mode. A current of 10 A was passed through the cell for 0.2 s followed by 0.8 s of zero current for the current cycle. The cell voltage was ~2.4 V, for an average input power of 4.8 W. The electrolysis power average was 1.84 W, and the stirrer power was measured to be 0.3 W. Thus, the total average net input power was 2.14 W. The cell was operated at various resistance heater settings, and the temperature difference between the cell and the ambient as well as the heater power was measured. The results of the excess power as a function of cell temperature with the cell operating in the pulsed power mode at 1 Hz with a cell voltage of 2.4 V, a peak power mode at 1 Hz with a cell voltage of 2.4 V, a peak current of 10 A, and a duty cycle of 20% showed that the excess power is temperature dependent for pulsed power operation, and the maximum excess power was 18 W for an input electrolysis joule heating power of 2.14 W. Thus, the ratio of excess power to input electrolysis joule heating power was 850%.

II.B. Sample Preparation

Sample 1: The sample was prepared by concentrating the K_2CO_3 electrolyte from the Thermacore electrolytic cell using a rotary evaporator at 50°C until a yellow-white polymeric suspension formed. The poly-yellow-white polymeric suspension formed. The polymeric material was observed after the volume had been reduced from 3000 to 150 cm³. The inorganic polymeric material was centrifuged to form a pellet that was collected following decanting of the concentrated electrolyte.

Sample 2: The sample was prepared by concentrating the K_2CO_3 electrolyte from the Thermacore electrolytic cell at room temperature using an evaporation dish until a yellow-white solid containing a polymeric material just formed. The remaining electrolyte was decanted, and the solid was dried and collected.

Sample 3: The sample was prepared by concentrating 300 cm³ of the K_2CO_3 electrolyte from the BLP electrolytic cell using a rotary evaporator at 50°C until a precipitate just formed. The volume was ~50 cm³. Additional electrolyte was added while heating at 50°C until the crystals disappeared. Crystals were then grown over 3 weeks by allowing the saturated solution to stand in a sealed round-bottom flask at 25°C. The yield was 1 g.

Sample 4: The cathode of the INEL electrolytic cell was placed in 28 ℓ of 0.6 M K_2CO_3/10% H_2O_2; 200 cm^3 of the solution was acidified with HNO_3. The solution was allowed to stand open for 3 months at room temperature in a 250-ml beaker. White nodular crystals formed on the walls of the beaker by a mechanism equivalent to thin layer chromatography involving atmospheric water vapor as the moving phase and the Pyrex silica of the beaker as the stationary phase.

Sample 5: The sample was prepared by filtering the K_2CO_3 electrolyte from the BLP electrolytic cell with a Whatman 110-mm filter paper.[c]

Sample 6: The reference consisted of K_2CO_3 (99%).

Sample 7: The reference consisted of $KHCO_3$ (99.99%).

Sample 8: The reference consisted of HNO_3 (99.99%).

II.C. TOF-SIMS Characterization

Samples were sent to Evans East (East Windsor, New Jersey) for TOF-SIMS analysis. The crystalline samples were sprinkled onto the surface of double-sided adhesive tapes and characterized using a Physical Electronics TFS-2000 TOF-SIMS instrument. The primary ion gun utilized a $^{69}Ga^+$ liquid metal source. To remove surface contaminants and expose a fresh surface, the samples were sputter cleaned for 30 s using a 40- $\times$ 40-μm raster. The aperture setting was 3, and the ion current was 600 pA, resulting in a total ion dose of 10^{15} ions/cm^2.

During acquisition, the ion gun was operated using a bunched (pulse width 4 ns bunched to 1 ns) 15-kV beam.[4,5d] The total ion dose was 10^{12} ions/cm^2. Charge neutralization was active, and the postaccelerating voltage was 8000 V. Three different regions on each sample of (12 μm)^2, (18 μm)^2, and (25 μm)^2 were analyzed. The positive and negative TOF-SIMS spectra were acquired. Representative postsputtering data are reported except where indicated.

II.D. XPS Characterization

The binding energy of various hydrino hydride ions may be obtained according to Eq. (3), as given in Table I. XPS was used to confirm the TOF-SIMS data showing production of the increased binding energy hydrogen compounds. This was achieved by identifying component hydrino hydride ions such as $n = \frac{1}{2}$ to $n = \frac{1}{16}$, $E_b = 3$ to 73 eV. The identities of the other elements of the samples were confirmed via the shifts of the primary element peaks of the component atoms due to binding with increased binding energy hydrogen species such as hydrino hydride ions. The hydrino hydride ion, $n = \frac{1}{16}$, is the most stable hydrino hydride ion. Thus, XPS of the energy range $E_b = 3$ to 73 eV detects these states. Compared to the

surface of a cathode as the sample, isolation of pure hydrino hydride compounds from the electrolyte is a means of eliminating impurities so that impurities are eliminated as an alternative assignment to the hydrino hydride ion peaks. The absence of impurities was determined from the survey spectrum over the region $E_b = 0$ to 1200 eV. The survey spectrum also detected shifts in the binding energies of elements bound to hydrino hydride ions.

A series of XPS analyses was made by the Zettlemoyer Center for Surface Studies, Sinclair Laboratory, Lehigh University, on the crystalline samples using a Scienta 300 XPS spectrometer. The fixed analyzer transmission mode and the sweep acquisition mode were used. The step energy in the survey scan was 0.5 eV, and the step energy in the high-resolution scan was 0.15 eV. In the survey scan, the time per step was 0.4 s, and the number of sweeps was 4. In the high-resolution scan, the time per step was 0.3 s, and the number of sweeps was 30. As the internal standard, C 1s at 284.6 eV was used.

II.E. Characterization by XRD

The X-ray diffraction (XRD) patterns were obtained by IC Laboratories (Amawalk, New York) using a Phillips 547 diffractometer tuned for CuK_α (1.540590-Å) radiation generated at 45 kV and 35 mA. The sample was scanned from 8 to 68 2-theta with a step size of 0.02 deg and 1 s/step.

II.F. FTIR Spectroscopy

Samples were transferred to an infrared transmitting substrate and analyzed by FTIR spectroscopy by Surface Science Laboratories (Mountain View, California) using a Nicolet Magna 550 FTIR spectrometer with a Nic-Plan FTIR microscope. The number of scans was 500 for both the sample and background. The number of background scans was 500. The resolution was 8.000. A dry air purge was applied.

II.G. Raman Spectroscopy

Experimental and control samples were analyzed blindly by the Environmental Catalysis and Materials Laboratory of Virginia Polytechnic Institute. Raman spectra were obtained with a Spex 500 M spectrometer coupled with a liquid nitrogen–cooled charge coupled device detector (Spectrum One, Spex). An Ar^+ laser (Model 95, Lexel) with a light wavelength of 514.5 nm was used as the excitation source, and a holographic filter (Super-Notch Plus, Kaiser) was employed to effectively reject the elastic scattering from the sample. The spectra were taken at ambient conditions, and the samples were placed in capillary glass tubes (0.8- to 1.1-mm outside diameter, 90 mm long, Kimble) on a capillary sample holder (Model 1492, Spex). Spectra of the powder samples were

---

[c]The Whatman filter paper is catalog number 1450110.
[d]Recent specifications are listed in Ref. 5.

acquired using the following condition: The laser power at the sample was 10 mW; the slit width of the monochromator was 20 mm, which corresponds to a resolution of 3 cm^{-1}; the detector exposure time was 10 s; and 30 scans were averaged.

II.H. NMR Spectroscopy

The ^{1}H MAS NMR was performed on the crystalline samples by Spectral Data Services (Champaign, Illinois). The data were obtained on a custom-built spectrometer operating with a Nicolet 1280 computer. Final pulse generation was from a tuned Henry radio amplifier. The ^{1}H NMR frequency was 270.6196 MHz. A 2-μs pulse corresponding to a 15-deg pulse length and a 3-s recycle delay was used. The window was ±31 kHz. The spin speed was 4.5 kHz. The number of scans was 1000. Chemical shifts were referenced to external TMS. The offset was 1527.12 Hz, and the magnetic flux was 6.357 T.

III. RESULTS AND DISCUSSION

III.A. TOF-SIMS

The positive TOF-SIMS spectrum obtained from the KHCO$_3$ control is shown in Figs. 1 and 2. Moreover, the positive TOF-SIMS of sample 1 isolated from the electrolytic cell is shown in Figs. 3 and 4. The respective hydride compounds and mass assignments appear in Table II. In both the control and sample 1, the positive ion spectrum is dominated by the K$^+$ ion. Two series of positive ions $\{K[K_2CO_3]_n^+$ $m/z = (39 + 138n)$ and $K_2OH[K_2CO_3]_n^+$ $m/z = (95 + 138n)\}$ are
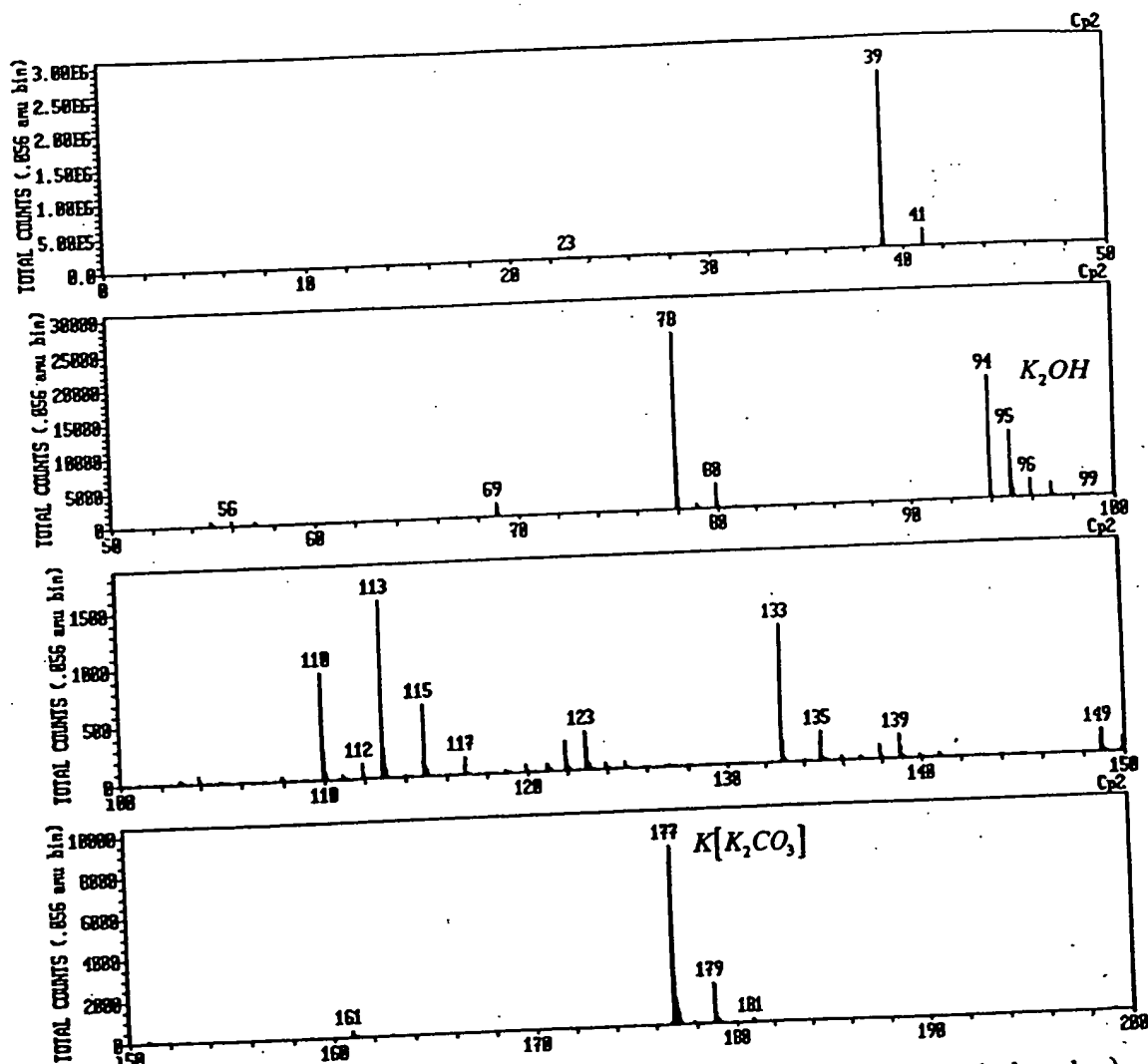

Fig. 1. The positive TOF-SIMS spectrum (m/e = 0 to 200) of 99.99% KHCO$_3$ (HC = hydrocarbon).
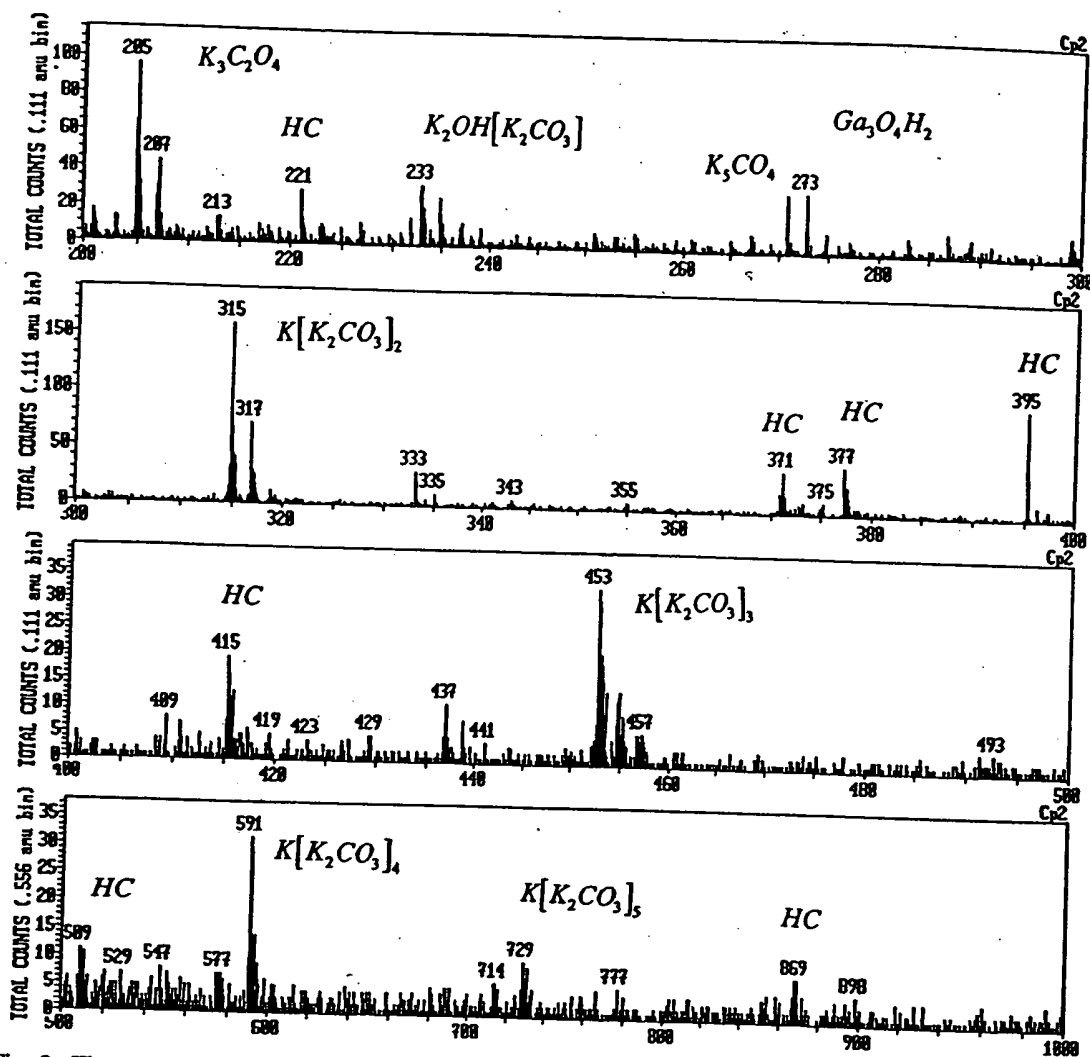
Fig. 2. The positive TOF-SIMS spectrum (m/e = 200 to 1000) of 99.99% KHCO$_3$ (HC = hydrocarbon).

observed in the KHCO$_3$ control. Other peaks containing potassium include KC^+, $K_xO_y^+$, $K_xO_yH_z^+$, KCO^+, and K_2^+. However, in sample 1, three new series of positive ions are observed at $\{K[KH\ KHCO_3]_n^+\ m/z = (39 + 140n)$, $K_2OH[KH\ KHCO_3]_n^+\ m/z = (95 + 140n)$, and $K_3O[KH\ KHCO_3]_n^+\ m/z = (133 + 140n)\}$. These ions correspond to inorganic clusters containing novel hydride combinations (i.e., KH KHCO$_3$ units plus other positive fragments). These 140 series peaks were also present in the positive TOF-SIMS spectrum of samples 2 and 3. The TOF-SIMS peaks of sample 1 were much more intense because of purification.

The comparison of the positive TOF-SIMS spectrum of the KHCO$_3$ control with the electrolytic cell sample shown in Figs. 1 and 2, and 3 and 4, respectively, demonstrates that the $^{39}K^+$ peak of sample 1 may saturate the detector and give rise to a peak that is atypical of the natural abundance of ^{41}K. The natural abundance of ^{41}K is 6.7%, whereas the observed ^{41}K

abundance from sample 1 is 57%. This atypical abundance was also confirmed using electrospray ionization time of flight mass spectroscopy[1] (ESITOFMS). The high-resolution mass assignment of the $m/z = 41$ peak of the electrolytic sample was consistent with ^{41}K, and no peak was observed at $m/z = 42.98$, ruling out $^{41}KH_2^+$. Moreover, the natural abundance of ^{41}K was observed in the positive TOF-SIMS spectra of KHCO$_3$, KNO$_3$, and KI standards that were obtained with an ion current such that the ^{39}K peak intensity was an order of magnitude higher than that given for sample 1. The saturation of the ^{39}K peak of the positive TOF-SIMS spectrum by the electrolytic cell sample 1 is indicative of a unique crystalline matrix.[6]

The respective hydride compounds and mass assignments of the negative ion TOF-SIMS of electrolytic cell sample 1 appear in Table III. The spectrum was dominated by H^- with much smaller O^-, and OH^- peaks. A series of nonhydride-containing negative ions
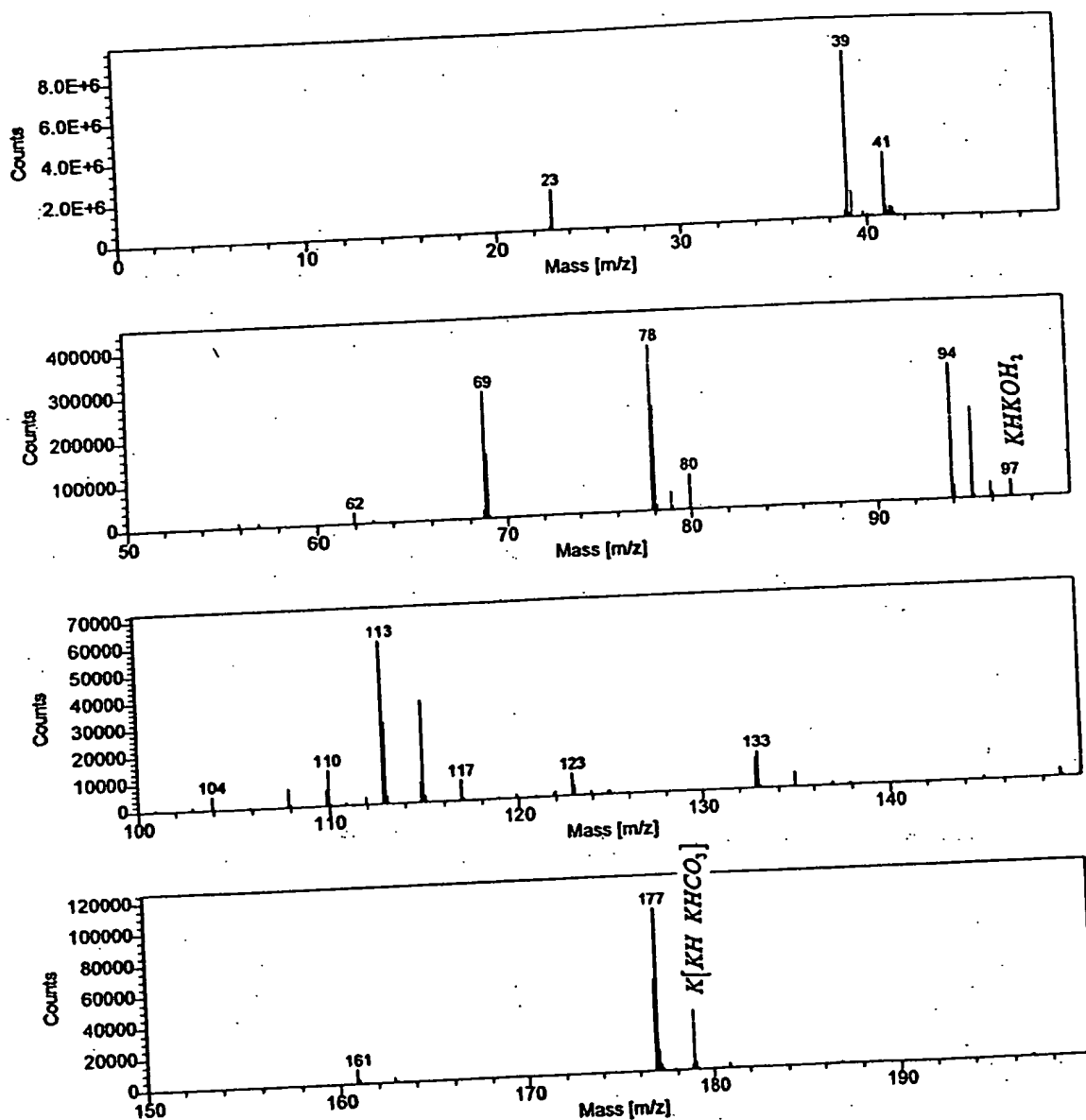
162

Fig. 3. The positive TOF-SIMS spectrum ($m/e = 0$ to 200) of the polymeric material prepared by concentrating the K_2CO_3 electrolyte from the Thermacore electrolytic cell with a rotary evaporator and centrifuging the polymeric material (sample 1) (HC = hydrocarbon).

{$KCO_3[K_2CO_3]_n^-$ $m/z = (99 + 138n)$} was also present, which implies that the hydride is lost with the proton during fragmentation of the compound KH KHCO$_3$. A photograph of the inorganic polymeric material suspended in distilled water is shown in Fig. 5.

Magnesium hydrino hydride ions MgH$_3^-$ ($m/e = 27.008515$) and Mg$_2$H$_4^-$ ($m/e = 52.00138$) were observed in the negative TOF-SIMS spectrum of sample 1. In sample 1, MgH$_3^-$ ($m/e = 27.008515$) was observed in the TOF-SIMS spectrum with a hydrocarbon peak at $m/e = 27.03$, and CN$^-$ was observed at $m/e = 26.00$, as shown in Fig. 6. Sample 1 was sput-

tered to remove hydrocarbons. The postsputtering negative TOF-SIMS spectrum $m/e = 20$ to 30 of sample 1 is shown in Fig. 7. The hydrino hydride compounds NaH$_3^-$ ($m/e = 26.013275$) and MgH$_3^-$ ($m/e = 27.008515$) were observed at $m/e = 26.01$ and $m/e = 27.01$, respectively.

The negative TOF-SIMS spectrum ($m/e = 10$ to 20) of 99.99% KHCO$_3$ is shown in Fig. 8. The negative TOF-SIMS spectrum ($m/e = 10$ to 20) of sample 1 is shown in Fig. 9. The negative TOF-SIMS spectrum ($m/e = 10$ to 20) of sample 4 is shown in Fig. 10. A peak with a high nominal mass that does not match any known compound
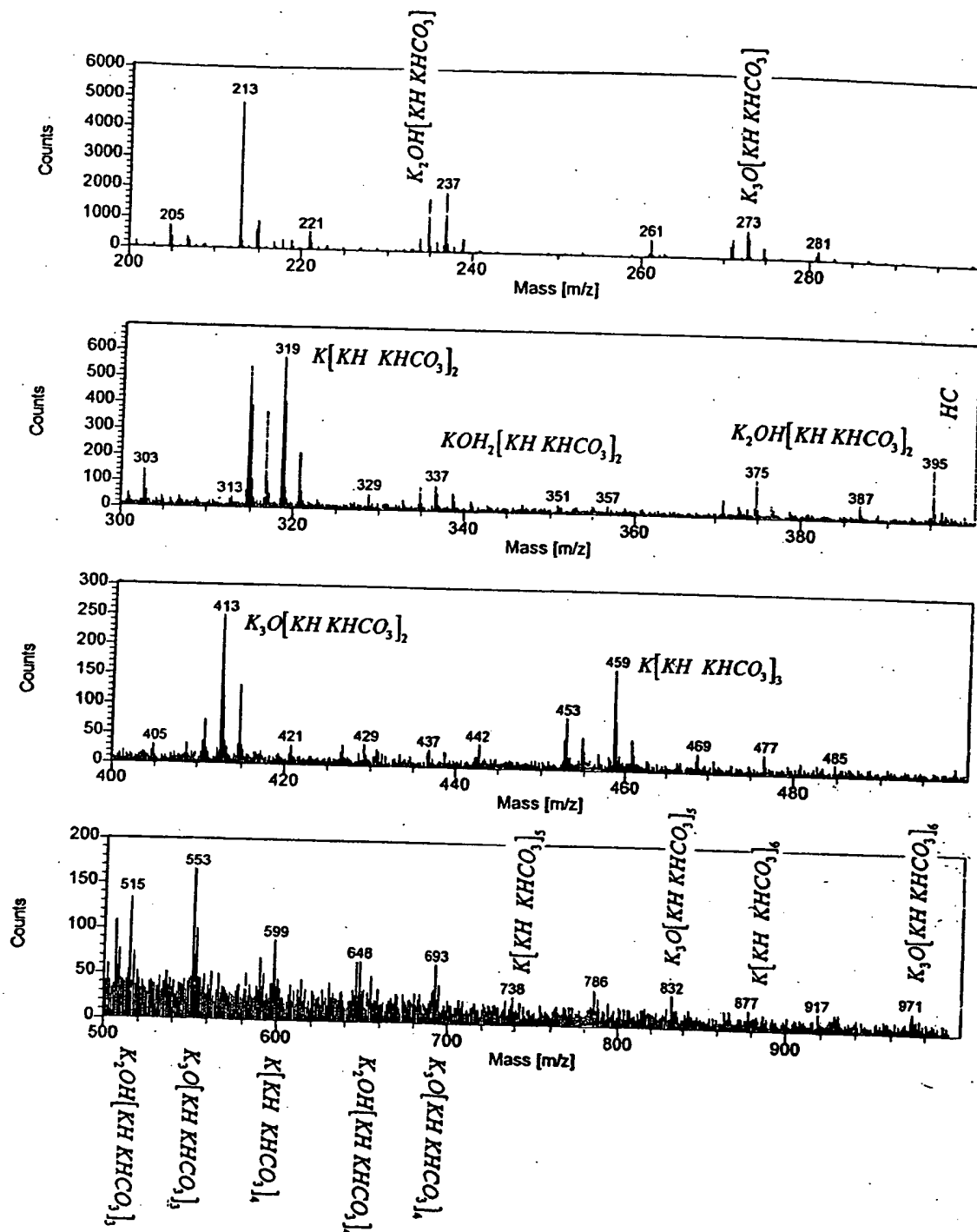
163

Fig. 4. The positive TOF-SIMS spectrum (m/e = 200 to 1000) of polymeric material prepared by concentrating the K_2CO_3 electrolyte from the Thermacore electrolytic cell with a rotary evaporator and centrifuging the polymeric material (sample 1) (HC = hydrocarbon).

or fragment was observed at m/e = 16.125 in the case of sample 1 and at m/e = 16.130 in the case of sample 4. Each mass excess peak has the same width as the oxygen peak; thus, each is not a metastable peak. Each peak is

not due to detector ringing because no such peak with a high nominal mass is seen at the position of any of the other identifiable peaks such as hydroxyl (OH) at m/e = 17.003, which has a greater intensity, and the peaks were

164

TABLE II

The Respective Hydride Compounds and Mass Assignments (m/z) of the Positive TOF-SIMS of Sample 1

Hydrino Hydride Compound or Fragment	Nominal Mass m/e	Observed m/e	Calculated m/e	Difference Between Observed and Calculated m/e
H_{23}	23	23.180	23.179975	0.000
NaH	24	23.99	23.997625	0.008
OH_{23}	39	39.178	39.174885	0.003
KH	40	39.97	39.971535	0.0015
NaHKH	64	63.96	63.96916	0.009
K_2H	79	78.940	78.935245	0.004
$(KH)_2$	80	79.942	79.94307	0.001
K_2H_5	83	82.96	82.966545	0.007
$KHKOH_2$	97	96.945	96.945805	0.0008
KKHNaH	103	102.93	102.93287	0.003
$KH_2(KH)_2$	121	120.925	120.92243	0.003
$KH\ KHCO_2$	124	123.925	123.93289	0.008
KH_2KHO_4	145	144.92	144.930535	0.010
$K(KOH)_2$	151	150.90	150.8966	0.003
$KH(KOH)_2$	152	151.90	151.904425	0.004
$KH_2(KOH)_2$	153	152.90	152.91225	0.012
$K[KH\ KHCO_3]$	179	178.89	178.8915	0.001
$KCO(KH)_3$	187	186.87	186.873225	0.003
$K_2OHKHKOH$	191	190.87	190.868135	0.002
$KH_2KOHKHKOH$	193	192.89	192.883785	0.006
$K_3O(H_2O)_4$	205	204.92	204.92828	0.008
$K_2OH[KH\ KHCO_3]$	235	234.86	234.857955	0.002
$K[H_2CO_4KH\ KHCO_3]$	257	256.89	256.8868	0.003
$K_3O[KH\ KHCO_3]$	273	272.81	272.81384	0.004
$[KH_2CO_3]_3$	303	302.88	302.89227	0.012
$K[KH\ KHCO_3K_2CO_3]$	317	316.80	316.80366	0.004
$K[KH\ KHCO_3]_2$	319	318.82	318.81931	0.001
$KH_2[KH\ KOH]_3$	329	328.80	328.7933	0.007
$KOH_2[KH\ KHCO_3]_2$	337	336.81	336.82987	0.020
$KH\ KO_2[KH\ KHCO_3][KHCO_3]$	351	350.81	350.80913	0.001
$KKHK_2CO_3[KH\ KHCO_3]$	357	356.77	356.775195	0.005
$KKH[KH\ KHCO_3]_2$	359	358.78	358.790845	0.011
$K_2OH[KH\ KHCO_3]_2$	375	374.78	374.785755	0.005
$K_2OH[KHKOH]_2[KHCO_3]$	387	386.75	386.76238	0.012
$KKH_3KH_5[KH\ KHCO_3]_2$	405	404.79	404.80933	0.019
$K_3O[K_2CO_3][KH\ KHCO_3]$ or $K[KH\ KOH(K_2CO_3)_2]$	411	410.75	410.72599	0.024
$K_3O[KH\ KHCO_3]_2$	413	412.74	412.74164	0.002
$K[KH\ KOH(KH\ KHCO_3)_2]$	415	414.74	414.75729	0.017
$KH_2OKHCO_3[KH\ KHCO_3]_2$	437	436.81	436.786135	0.024
$KKHKCO_2[KH\ KHCO_3]_2$	442	441.74	441.744375	0.004
$K[KH\ KHCO_3]_3$	459	458.72	458.74711	0.027
$H[KH\ KOH]_2[K_2CO_3]_2$ or $K_4O_2H[KH\ KHCO_3]_2$	469	468.70	468.708085	0.008
$K[K_2CO_3][KHCO_3]_3$	477	476.72	476.744655	0.025
$K_2OH[KH\ KHCO_3]_3$	515	514.72	514.713555	0.006
$K_3O[KH\ KHCO_3]_3$	553	552.67	552.66944	0.001
$K[KH\ KHCO_3]_4$	599	598.65	598.67491	0.025
$K_2OH[KH\ KHCO_3]_4$	655	654.65	654.641355	0.009
$K_3O[KH\ KHCO_3]_4$	693	692.60	692.59724	0.003
$K[KH\ KHCO_3]_5$	739	738.65	738.60271	0.047
$K_3O[KH\ KHCO_3]_5$	833	832.50	832.52504	0.025
$K[KH\ KHCO_3]_6$	879	878.50	878.53051	0.031
$K_3O[KH\ KHCO_3]_6$	973	972.50	972.45284	0.047

TABLE III

The Respective Hydride Compounds and Mass Assignments (m/z) of the Negative TOF-SIMS of Sample 1

Hydrino Hydride Compound or Fragment	Nominal Mass m/e	Observed m/e	Calculated m/e	Difference Between Observed and Calculated m/e
H_{16}	16	16.130	16.1252	0.005
H_{24}	24	24.181	24.1878	0.007
H_{25}	25	25.195	25.195625	0.001
NaH_3	26	26.01	26.013275	0.003
MgH_3	27	27.01	27.008515	0.001
CH_{23}	35	35.183	35.179975	0.003
NH_{23}	37	37.185	37.183045	0.002
KH_3	42	42.00	41.987185	0.013
$(NaH)_2$	48	48.00	47.99525	0.005
Na_2H_3	49	49.00	49.003075	0.003
Mg_2H_4	52	52.00	52.00138	0.001
KH OH	57	56.98	56.97427	0.006
NaH_3 NaO	65	65.00	64.997985	0.002
NaH_2 KH_5	69	69.00	69.008285	0.008
$(KH)_2$	80	79.95	79.94307	0.007
KH KO	95	94.93	94.930155	0
KH_2KOH	97	96.945	96.945805	0.0008
GaKH	109	108.895	108.897235	0.002
KH KNO	109	108.923	108.933225	0.010
KH_3KCl	116	115.92	115.919745	0.000
$KOHNO_3$	118	117.95	117.954245	0.004
H_2I	129	128.92	128.92005	0.000
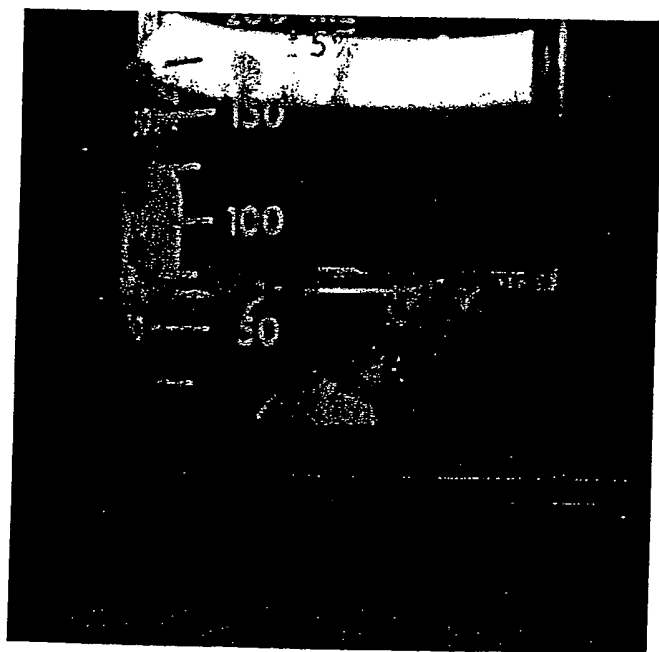
Fig. 5. Photograph of polymeric material comprising sample 1 suspended in distilled water.

repeatable using two different detectors. Also, they cannot be explained as an instrument artifact since each is present at the earliest times of acquisition. In both samples, the unidentifiable peak is assigned to polyhydrogen negative ion H_{16}^-, which is consistent with $H^-(\frac{1}{16})$ as the most stable hydrino hydride ion according to Eq. (3). The principal quantum number $p = 16$ provides 16 multipoles ($l = 0$ to $l = n - 1$) comprising the molecular orbitals of $H^-(\frac{1}{16})$. The agreement between the observed mass and the calculated mass ($m/e = 16.125$) is excellent. No other compound of this mass is possible.

Other positive and negative TOF-SIMS peaks observed for samples 1 and 4 confirm polyhydrogen compounds and ions. The positive TOF-SIMS spectrum ($m/e = 0$ to 50) of sample 4 is shown in Fig. 11. The positive TOF-SIMS spectrum ($m/e = 20$ to 30) of sample 1 is shown in Fig. 12. The presputtering negative TOF-SIMS spectrum ($m/e = 20$ to 30) of sample 1 is shown in Fig. 6. The postsputtering negative TOF-SIMS spectrum ($m/e = 30$ to 40) of sample 1 is shown in Fig. 13. The peak assigned to OH_{23}^+ ($m/e = 39.174885$) is shown in the positive TOF-SIMS spectrum of sample 4 (Fig. 11). The experimental mass is 39.175, which is in excellent agreement with the
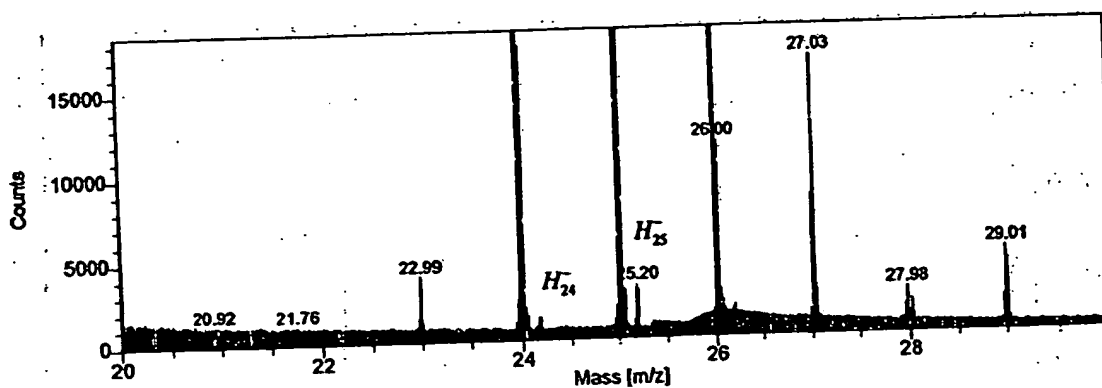
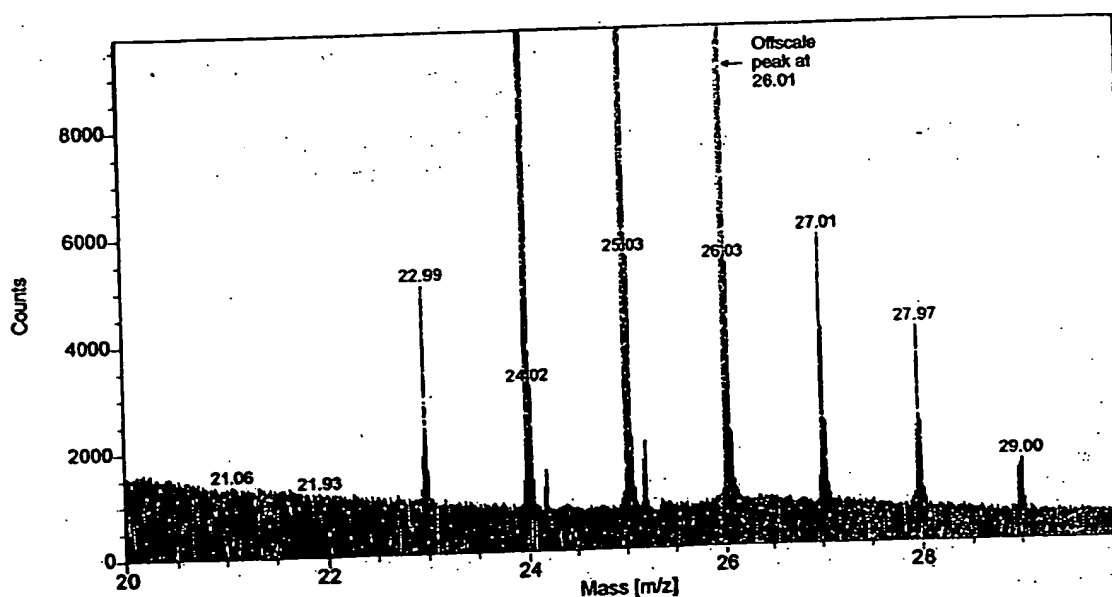Fig. 6. The presputtering negative TOF-SIMS spectrum (m/e = 20 to 30) of sample 1.

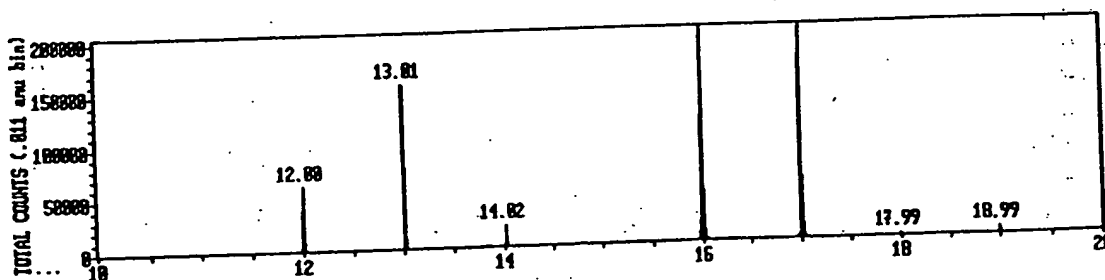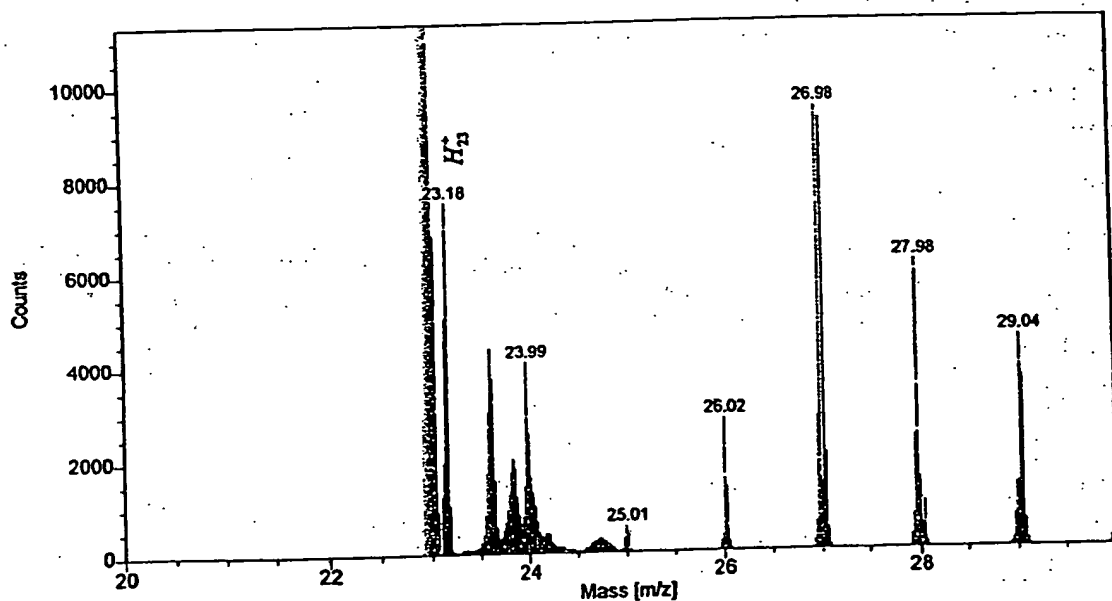Fig. 7. The postsputtering negative TOF-SIMS spectrum (m/e = 20 to 30) of sample 1.

Fig. 8. The negative TOF-SIMS spectrum (m/e = 10 to 20) of 99.99% $KHCO_3$.

calculated mass. The peak assigned to H_{23}^+ (m/e = 23.179975) is shown in the positive TOF-SIMS spectrum of sample 1 (Fig. 12). The experimental mass is 23.180. This peak is assigned to a fragment of a parent polyhydrogen molecule containing 24 hydrogen atoms. The corresponding negative ion, H_{24}^-, is shown in Fig. 6 with the M + 1 peak, H_{25}^-. These peaks are also observed in Fig. 7. Figures 11 and 14 show OH_{23}^+, which
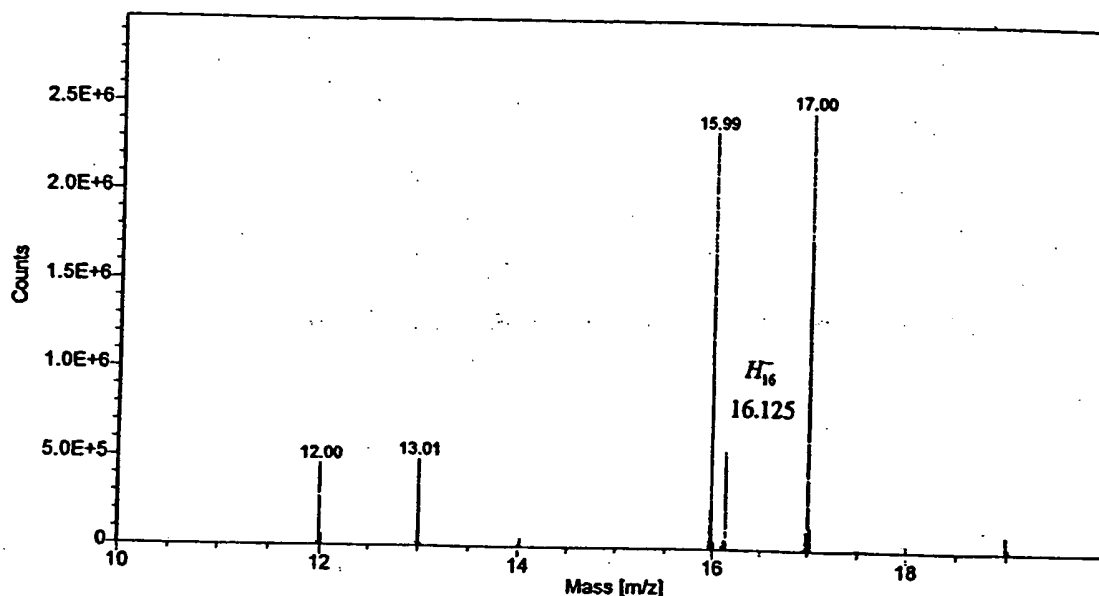
Fig. 9. The negative TOF-SIMS spectrum ($m/e = 10$ to 20) of polymeric material prepared by concentrating the K_2CO_3 electrolyte from the Thermacore electrolytic cell with a rotary evaporator and centrifuging the polymeric material (sample 1).
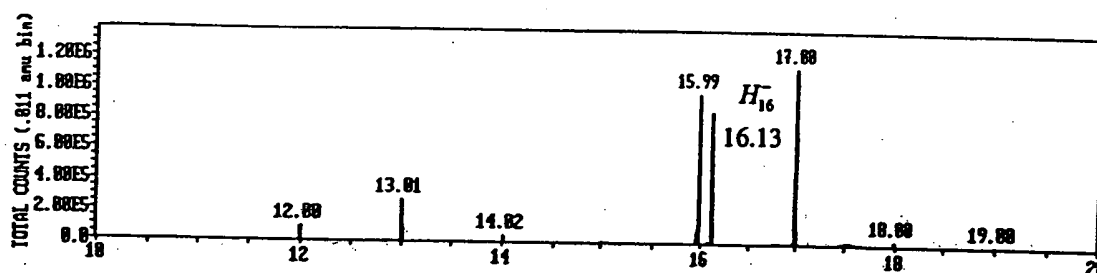
Fig. 10. The negative TOF-SIMS spectrum ($m/e = 10$ to 20) of crystals isolated from the cathode of the K_2CO_3 INEL electrolytic cell (sample 4).
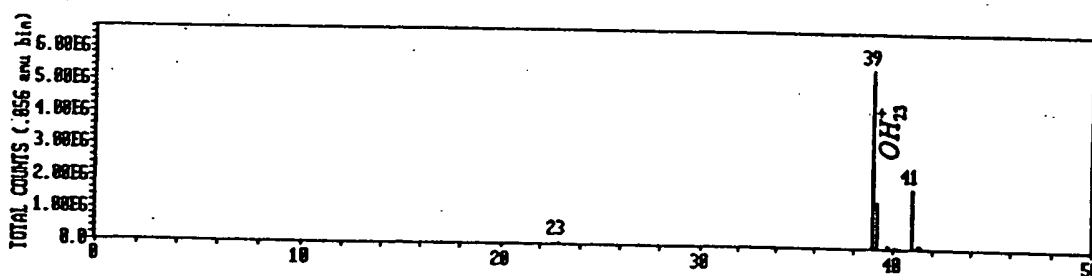
Fig. 11. The positive TOF-SIMS spectrum ($m/e = 0$ to 50) of sample 4.

may be a fragment of OH_{24}, and OH^- may also be a fragment. The OH^- ($m/e = 17.002735$) peak intensity of the negative spectrum of sample 4 shown in Fig. 10 is at least twice that of the control. The increased intensity is as-

signed to the fragmentation of OH_{24} to OH^-. In addition to substitution reactions with oxygen, the 24-atom polyhydrogen molecule may react with carbon and nitrogen. The negative ions CH_{23}^- and NH_{23}^- are shown in Fig. 13.

Fig. 12. The positive TOF-SIMS spectrum (m/e = 20 to 30) of sample 1.
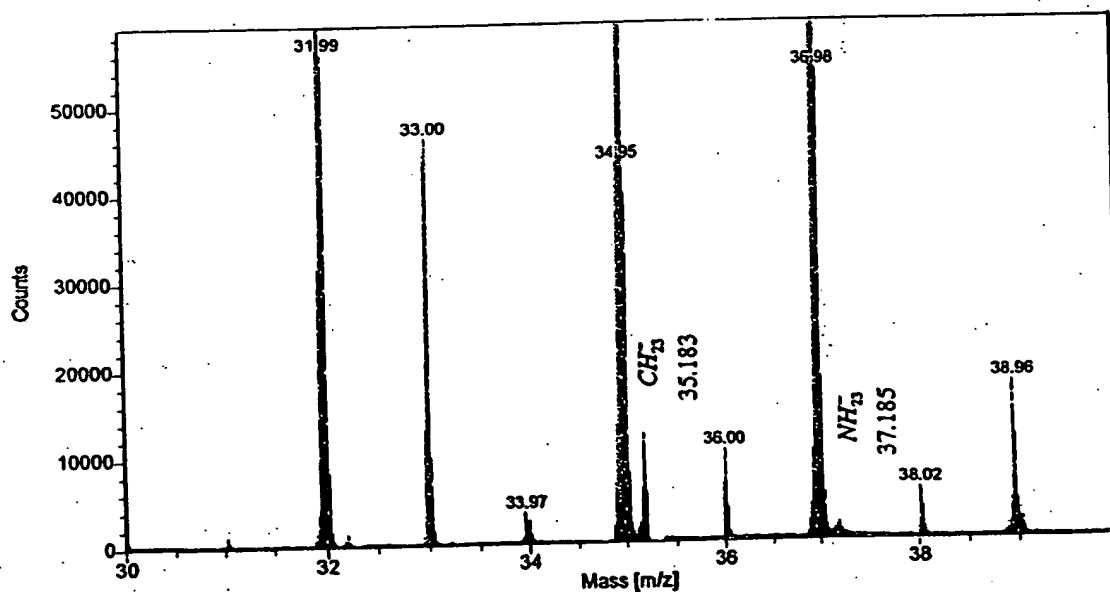
Fig. 13. The postsputtering negative TOF-SIMS spectrum (m/e = 30 to 40) of sample 1.

Polymer compounds and ions comprising 24 hydrogen atoms may form because H_{24}^- is the last stable hydride ion of the series $1/p$ = 1 to $1/24$ given by Eq. (3). The most stable hydride ion that may give rise to compounds and ions containing 16 hydrogen atoms is H_{16}^-. Positive polyhydrogen ion peaks observed from the TOF-SIMS spectrum of sample 1 are given in Table II. Negative polyhydrogen ion peaks observed from the TOF-SIMS spectrum of sample 1 are given in Table III.

III.B. X-Ray Photoelectron Spectroscopy

A survey spectrum was obtained over the region E_b = 0 to 1200 eV. The primary element peaks allowed for the determination of all of the elements present in each sample isolated from the K_2CO_3 electrolyte. The survey spectrum also detected shifts in the binding energies of the' elements, which had implications as to the identity of the compound containing the elements. A high-resolution XPS
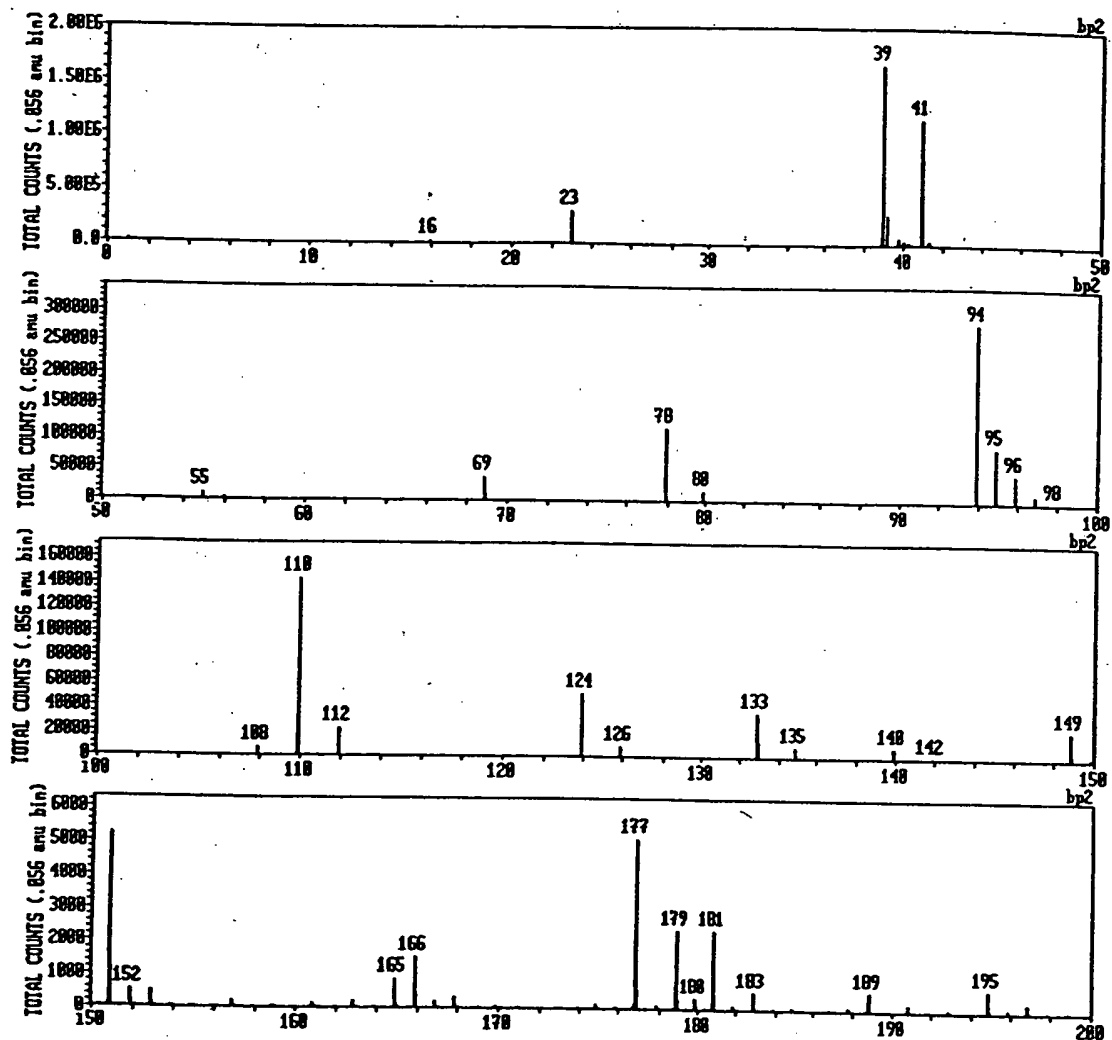
Fig. 14. The positive TOF-SIMS spectrum ($m/e = 0$ to 200) of crystals isolated from the cathode of the K_2CO_3 INEL electrolytic cell (sample 5).

spectrum was also obtained of the low binding energy region ($E_b = 0$ to 100 eV) to determine the presence of novel XPS peaks.

Samples 2 and 3 were purified from the K_2CO_3 electrolyte of the Thermacore and BLP electrolytic cells, respectively. No elements are present in the survey scans that can be assigned to peaks in the low binding energy region with the exception of a small variable contaminant of sodium at 64 and 31 eV, potassium at 16.2 and 32.1 eV, and oxygen at 23 eV. Accordingly, any other peaks in this region must be due to novel compositions. The theoretical positions of hydrino hydride ion peaks $H^-(n = 1/p)$ for $p = 2$ to $p = 16$ are identified for each of samples 2 and 3 in Figs. 15 and 16, respectively. The O $2s$, which is weak compared to the potassium peaks of K_2CO_3, is typically present at 23 eV but is broad or obscured in Figs. 15 and 16. In addition, the sodium peaks

Na of sample 3 are identified in Fig. 16. The K $3s$ and K $3p$, K, are shown in Figs. 15 and 16 at 16.2 and 32.1 eV, respectively. Peaks centered at 22.8 and 38.8 eV, which do not correspond to any other primary element peaks, were observed. The intensity and shift match shifted K $3s$ and K $3p$. Hydrogen is the only element that does not have primary element peaks; thus, it is the only candidate to produce the shifted peaks. These peaks may be shifted by a novel hydride ion with a high binding energy of 22.8 eV that bonds to potassium K $3p$ and shifts the peak to this energy. In this case, the K $3s$ is similarly shifted. The XPS peaks centered at 22.8 and 38.8 eV are assigned to shifted K $3s$ and K $3p$. The anion does not correspond to any other primary element peaks; thus, it may correspond to the $H^-(n = \frac{1}{6})E_b = 22.8$ eV hydride ion predicted by Mills,[1] where E_b is the predicted binding energy. These peaks were not present in the case of
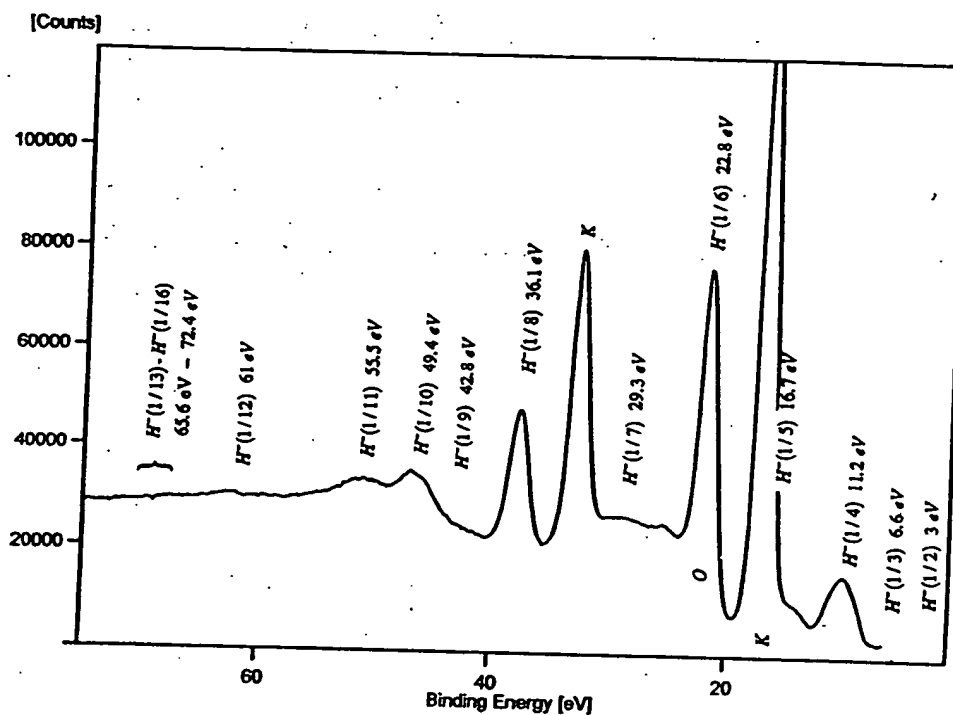
Fig. 15. The 0- to 80-eV binding energy region of a high-resolution XPS of polymeric material prepared by concentrating the K_2CO_3 electrolyte from the Thermacore electrolytic cell until a precipitate just formed (sample 2) with the primary elements identified.
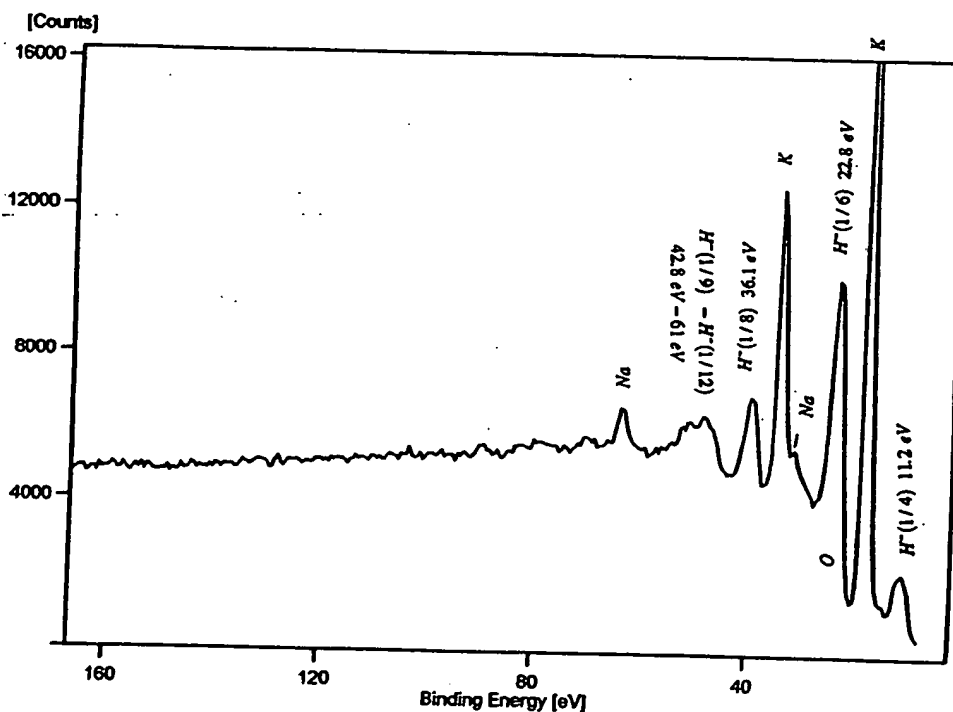

Fig. 16. The 0- to 165-eV binding energy region of the survey XPS of crystals prepared by concentrating the K_2CO_3 electrolyte from the BLP electrolytic cell with a rotary evaporator and allowing crystals to form on standing at room temperature (sample 3) with the primary elements identified.

the XPS of matching samples isolated from an identical electrolytic cell except that Na_2CO_3 replaced K_2CO_3 as the electrolyte.

XPS further confirmed the TOF-SIMS data by showing shifts of the primary elements. The splitting of the principal peaks of the survey XPS spectrum of samples 2 and 3 indicative of multiple forms of bonding involving the atom of each split peak appear in Table IV. The selected survey spectra with the corresponding figures of the high-resolution spectra of the low binding energy region are given as (#/#). The latter contain hydrino hydride ion peaks. And, several of the shifts of the peaks of elements given in Table IV and shown in the survey spectra are greater than those of known compounds. For example, the XPS survey spectrum of sample 3, which appears in Fig. 17, shows extraordinary potassium and oxygen peak shifts. All of the potassium primary peaks are shifted to about the same extent as that of the K $3s$ and K $3p$. In addition, extraordinary O $1s$ peaks of the electrolytic cell sample were observed at 537.5 and 547.8 eV, whereas a single O $1s$ was observed in the XPS spectrum of K_2CO_3 at 532.0 eV. The results are not due to uniform charging as the internal standard C $1s$ remains the same at 284.6 eV. Also, the results are not due to differential charging because the peak shapes of carbon and oxygen are normal, and no tailing of these peaks was observed. The range of binding energies from the literature[7] for the peaks of interest is given in the final

row of Table IV. The peaks shifted to an extent that they are without identifying assignment correspond to and identify compounds containing hydrino hydride ions. For example, the positive and negative TOF-SIMS spectra of sample 3 were similar to that of sample 1 (Tables II and III). The spectrum contained inorganic hydride clusters

$$(K[KH\ KHCO_3]_n^+\ m/e = (39 + 140n)\ ,$$

$$K_2OH[KH\ KHCO_3]_n^+\ m/e = (95 + 140n)\ ,$$

and

$$K_3O[KH\ KHCO_3]_n^+\ m/e = (133 + 140n))$$

observed in the positive TOF-SIMS spectrum of sample 1. In addition, the positive TOF-SIMS spectra of sample 3 showed large peaks, which were identified as KHKOH and $KHKOH_2$, as shown in Fig. 18. The extraordinary shifts of the K $3p$, K $3s$, K $2p_3$, K $2p_1$, and K $2s$ XPS peaks and the O $1s$ XPS peak shown in Fig. 17 are assigned to novel hydride compounds. TOF-SIMS and XPS taken together provide substantial support of hydrino hydride compounds as assigned herein.

The 0- to 60-eV binding energy region of a high-resolution XPS spectrum of crystals isolated from the INEL electrolytic cell (sample 4) with the primary element peaks identified appears in Fig. 19. No elements were present in the survey scan that can be assigned to

TABLE IV

The Binding Energies of XPS Peaks of K_2CO_3 and Electrolytic Cell Samples

| XPS #	FIG #	C $1s$ (eV)	N $1s$ (eV)	O $1s$ (eV)	Na $1s$ (eV)	K $3p$ (eV)	K $3s$ (eV)	K $2p_3$ (eV)	K $2p_1$ (eV)	K $2s$ (eV)
K_2CO_3		284.6 288.4		532.0		18	34	292.4	295.2	376.7
2	15	284.6 288.8	~390 Very broad	530.7 537.3 547.5	1070.0	16.2 22.8	32.1 38.8	291.5 298.5	293.7 300.4	376.6 382.6
3	17 16	284.6 288.5	393.6	530.9 537.5 547.8	1070.0	16.2 22.8	32.1 38.8	291.5 298.5	293.7 300.4	376.6 382.6
4	19	284.6 288.2	403.2 407.4	530.3 532.2 540.6 545.2	1070.8	16.8	32.7	295.3	292.6	377.5
5	20 21	284.6 285.7 287.4 288.7	403.2 407.0	532.1 535.7 563.8	1070.9 1077.5					
Minimum Maximum		280.5 293	398 407.5	529 535	1070.4 1072.8			292 293.2		
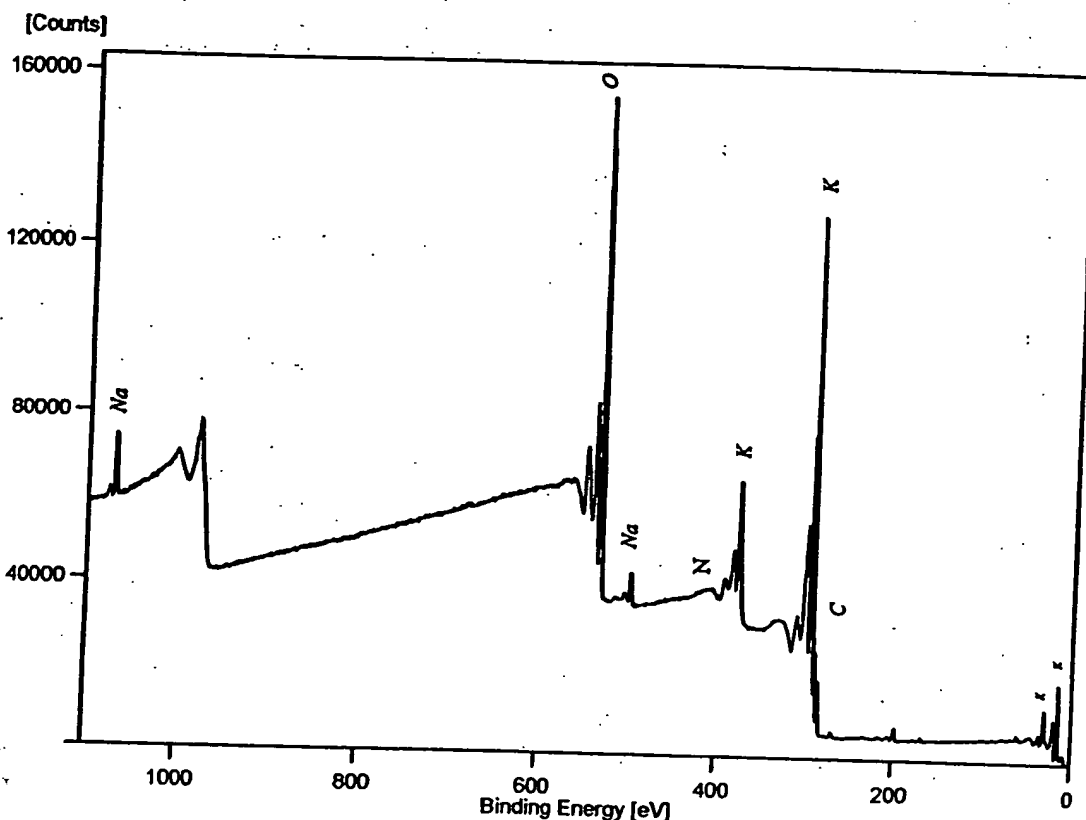
Fig. 17. The survey XPS of crystals prepared by concentrating the K_2CO_3 electrolyte from the BLP electrolytic cell with a rotary evaporator and allowing crystals to form on standing at room temperature (sample 3) with the primary elements identified.
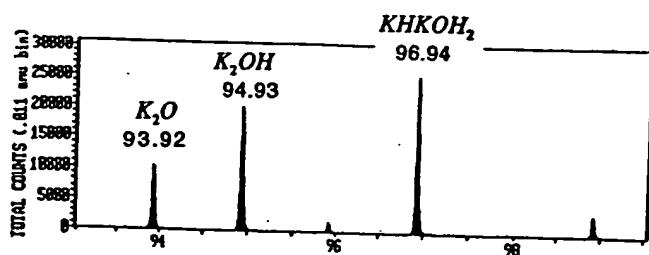

Fig. 18. The TOF-SIMS spectra ($m/e = 94$ to 99) of sample 3.

peaks in the low binding energy region with the exception of sodium at 64 and 31 eV, potassium at 16.8 and 32.7 eV, and oxygen at 23 eV. Accordingly, any other peaks in this region must be due to novel compositions. The theoretical positions of hydrino hydride ion peaks H^- $(\frac{1}{2})$ to H^- $(\frac{1}{11})$, as well as the weak oxygen peak, O 23 eV, sodium peaks, Na 31 eV and Na 64 eV, and the potassium peaks, K $3p$ and K $3s$, are identified for sample 4 in Fig. 19. The hydrino hydride peak $H^-(\frac{1}{5})$ 16.7 eV is

under the K $3p$ peak. The hydrino hydride peak $H^-(\frac{1}{7})$ 29.3 eV is under the Na 31 eV peak. These hydrino hydride ion features were not present in the case of the XPS of matching samples except that Na_2CO_3 replaced K_2CO_3 as the electrolyte. The XPS data confirm the TOF-SIMS data of increased binding energy hydrogen compounds.

The survey scan of sample 5 is shown in Fig. 20 with the primary elements identified. No elements are present in the survey scan that can be assigned to peaks in the low binding energy region, with the exception of sodium at 64 and 31 eV and oxygen at 23 eV. Accordingly, any other peaks in this region must be due to novel compositions. The theoretical positions of hydrino hydride ion peaks $H^-(n = 1/p)$ for $p = 2$ to $p = 16$ and the oxygen peak O and sodium peaks Na are identified for sample 5 in Fig. 21. These peaks were not present in the case of the XPS of matching samples except that Na_2CO_3 replaced K_2CO_3 as the electrolyte.

The data provide the identification of hydrino hydride ions whose XPS peaks cannot be assigned to impurities. Several of the peaks are split, such as the $H^-(n = \frac{1}{4})$, $H^-(n = \frac{1}{5})$, $H^-(n = \frac{1}{8})$, $H^-(n = \frac{1}{10})$, and $H^-(n = \frac{1}{11})$ peaks shown in Fig. 21. The splitting
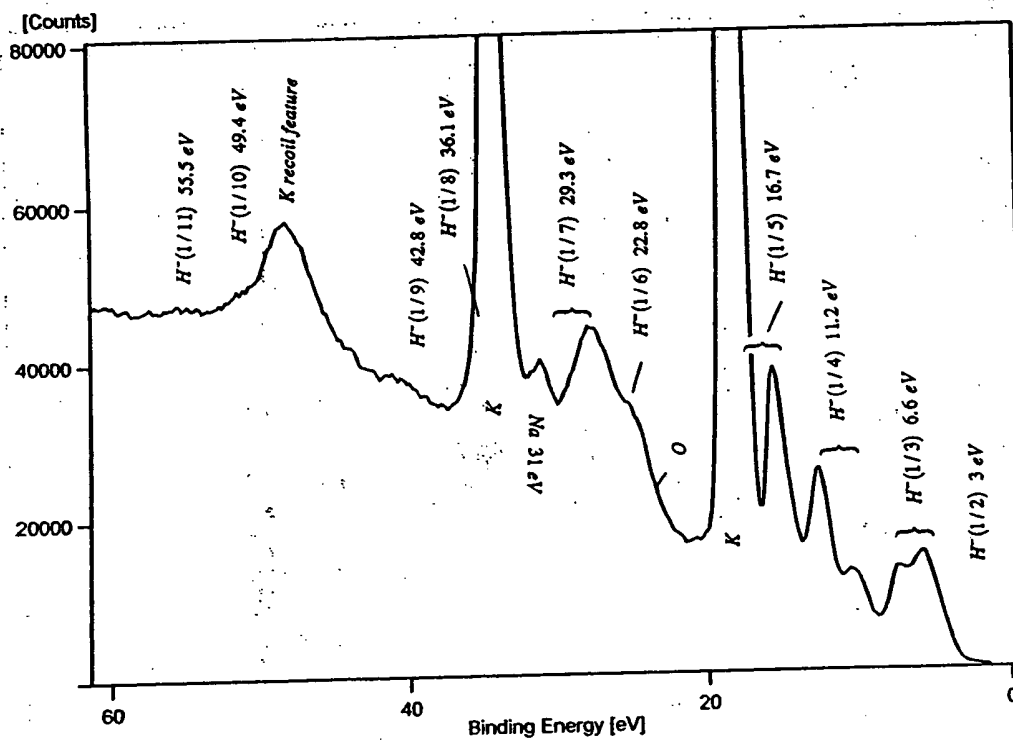
Fig. 19. The 0- to 60-eV binding energy region of a high-resolution XPS of crystals isolated from the K₂CO₃ INEL electrolytic cell (sample 4) with the primary element peaks identified.

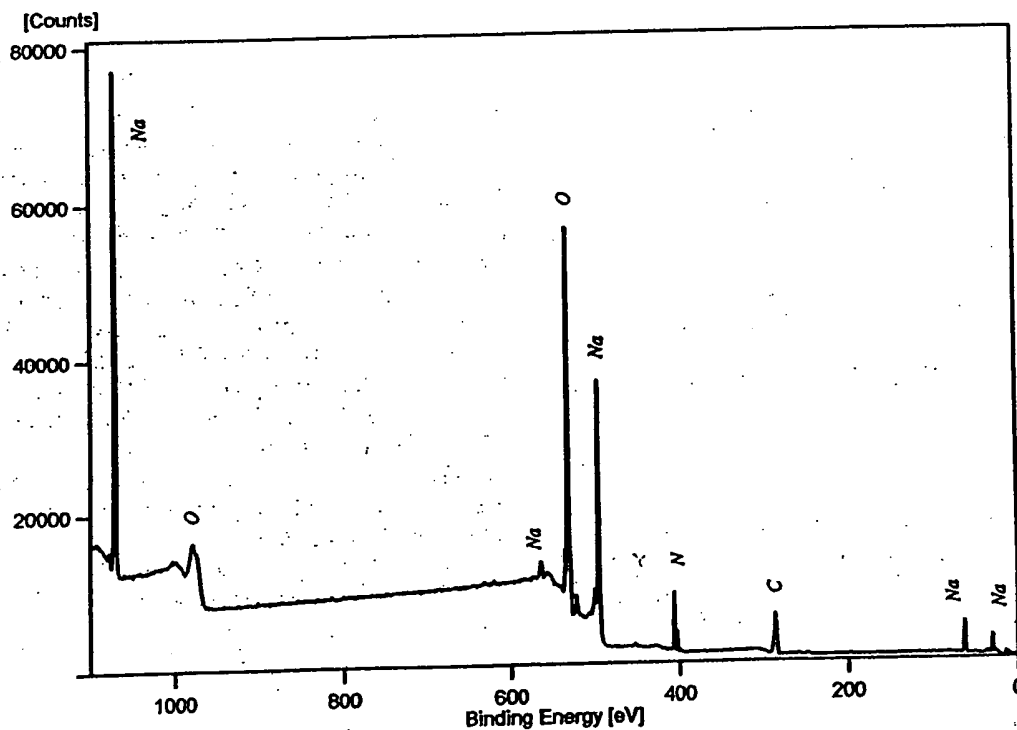

Fig. 20. The survey spectrum of crystals prepared by filtering the K₂CO₃ electrolyte from the BLP electrolytic cell (sample 5) with the primary elements identified.
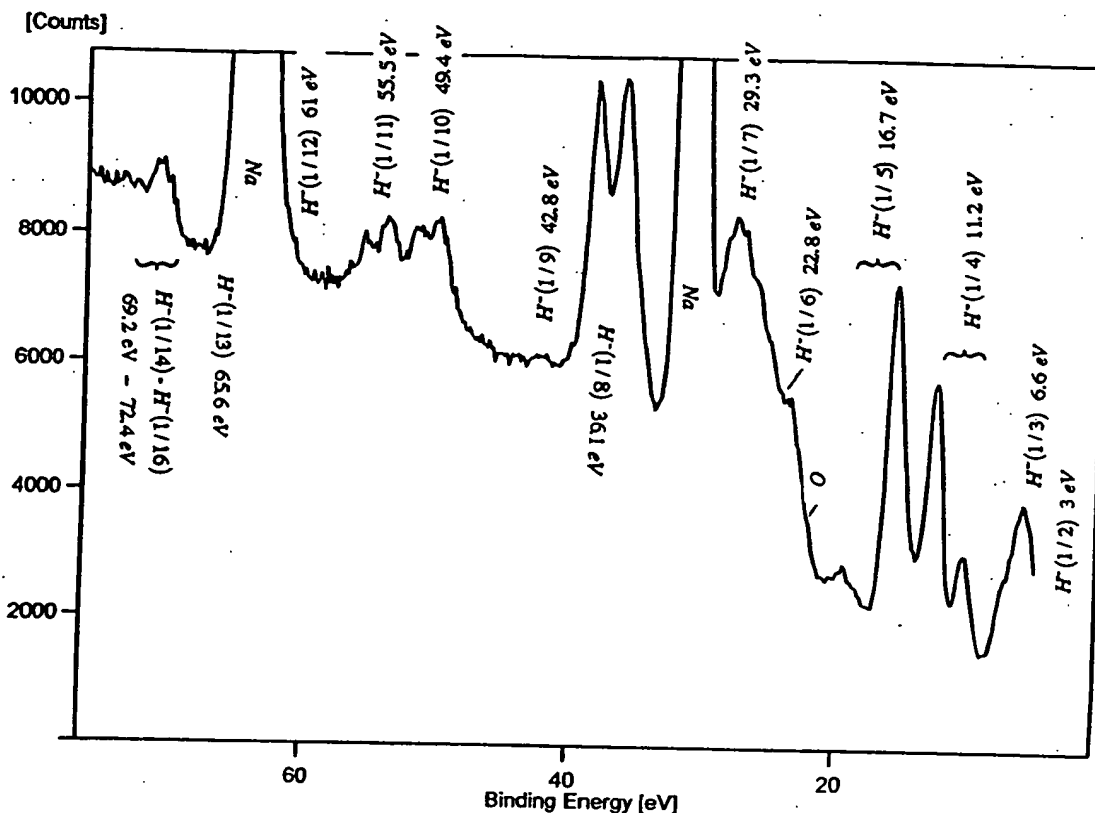
Fig. 21. The 0- to 75-eV binding energy region of a high-resolution XPS of crystals prepared by filtering the K_2CO_3 electrolyte from the BLP electrolytic cell (sample 5).

indicates that several compounds comprising the same hydrino hydride ion are present and that they may have different chemical environments.

The intensities of the corresponding peaks of the positive and negative TOF-SIMS were consistent with the majority compound and fragments comprising fragments of $NaNO_2$ > $NaNO_3$ and sodium hydrides. For example, NaH (m/e = 23.997625) and NaH_3 (m/e = 26.013275) were observed in the positive and negative TOF-SIMS, respectively, at (m/e = 23.99) and (m/e = 26.01). The observation by TOF-SIMS that the majority compound and fragments contain $NaNO_2$ > $NaNO_3$ is further confirmed by the presence of nitrite and nitrate nitrogen in the XPS spectrum (XPS sample 5 summarized in Table IV). The XPS Na $1s$ peak and the intensities of the N $1s$ peaks as nitrite (403.2 eV) greater than nitrate (407.4 eV) confirm the majority species as $NaNO_2$ > $NaNO_3$.

Sample 5 was filtered from an initially 0.57 M K_2CO_3 electrolyte. The solubility of NaOH is $42^{0^\circ C} \cdot g/100$ cm^3 (10.5 M). The solubility of $NaNO_2$ is $81.5^{15^\circ C} \cdot g/100$ cm^3 (11.8 M), and the solubility of $NaNO_3$ is $92.1^{25^\circ C} \cdot g/100$ cm^3 (10.8 M), whereas the solubility of K_2CO_3 is $112^{25^\circ C} \cdot g/100$ cm^3 (8.1 M) and the solubility of $KHCO_3$

is $22.4^{coldwater} \cdot g/100$ cm^3 (2.2 M) (Ref. 8). Thus, $NaNO_2$ and $NaNO_3$ as the filtered precipitate is unexpected. The solubility, TOF-SIMS, and XPS results support the assignment of sodium nitrite and nitrate hydrino hydride compounds that are less soluble than $KHCO_3$. General structures for these compounds are given by substitution of sodium for potassium in the structures given in Eq. (10).

III.C. X-Ray Diffraction

The X-ray diffraction (XRD) pattern of sample 2 is shown in Fig. 22. The XRD data indicated that the diffraction pattern of sample 2 does not match that of either KH, $KHCO_3$, K_2CO_3, or KOH. The identifiable peaks corresponded to a mixture of $K_4H_2(CO_3)_3 \cdot 1.5$ H_2O and $K_2CO_3 \cdot 1.5$ H_2O. In addition, the spectrum contained a number of peaks that could not be assigned. The 2-theta and d-spacings of the unidentified XRD peaks of sample 2 are given in Table V.

In addition, the elemental analysis of the crystals was obtained at Galbraith Laboratories. The atomic hydrogen percentage was in excess even if the compound were considered 100% $K_4H_2(CO_3)_3 \cdot 1.5$ H_2O, which would have the most hydrogen.
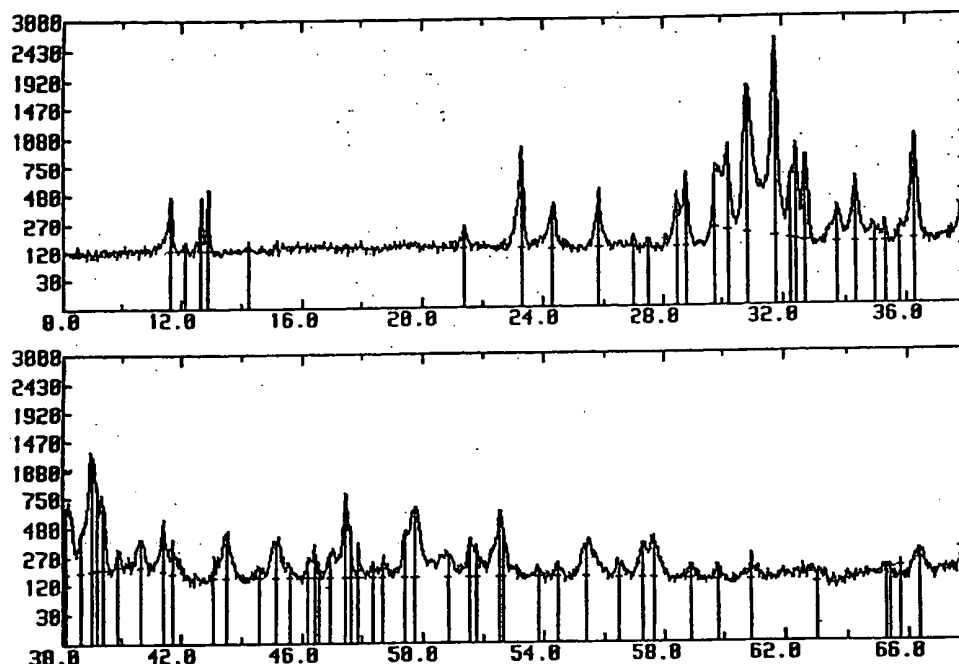
Fig. 22. The XRD pattern of polymeric material prepared by concentrating the K_2CO_3 electrolyte from the Thermacore electrolytic cell until a precipitate just formed (sample 2).

TABLE V

The 2-Theta and d-Spacings of the Unidentified XRD Peaks of the Crystals from K_2CO_3 Electrolytic Cell (Sample 2)

Peak Number	2-Theta (deg)	d (Å)
2	12.15	7.2876
4	12.91	6.8574
8	24.31	3.6614
12	28.46	3.1362
15	30.20	2.9594
31	39.34	2.2906
33	40.63	2.2206
36	43.10	2.0991
40	45.57	1.9905
42	46.40	1.9570
46	47.59	1.9141
47	47.86	1.9006
52	50.85	1.7958
54	51.75	1.7665
56	52.65	1.7386
57	53.81	1.7037
58	54.46	1.6850
60	56.49	1.6292
63	58.88	1.5685
65	60.93	1.5207
66	63.04	1.4747

III.D. Fourier Transform Infrared Spectroscopy

The FTIR spectra of K_2CO_3 (99%) and $KHCO_3$ (99.99%) were compared with that of sample 2. A spectrum of a mixture of the bicarbonate and the carbonate was produced by digitally adding the two reference spectra. The two standards alone and the mixed standards were compared with that of sample 2. From the comparison, it was determined that sample 2 contained potassium carbonate but did not contain potassium bicarbonate. The unknown component could be a bicarbonate other than potassium bicarbonate. The spectrum of potassium carbonate was digitally subtracted from the spectrum of sample 2. The subtracted spectrum appears in Fig. 23. Several bands were observed including bands in the 1400- to 1600-cm^{-1} region. Some organic nitrogen compounds (e.g., acrylamides and pyrolidinones) have strong bands in the region 1660 cm^{-1} (Ref. 9). However, the lack of any detectable C-H bands ($\approx$2800 to 3000 cm^{-1}) and the bands present in the 700- to 1100-cm^{-1} region indicate an inorganic material.[10] Peaks that are not assignable to potassium carbonate were observed at 3294, 3077, 2883, 1100, 2450, 1660, 1500, 1456, 1423, 1300, 1154, 1023, 846, 761, and 669 cm^{-1}.

The overlap FTIR spectrum of sample 2 and the FTIR spectrum of the reference potassium carbonate appear in Fig. 24. In the 700- to 2500-cm^{-1} region, the peaks of electrolytic cell sample 2 closely resemble those of
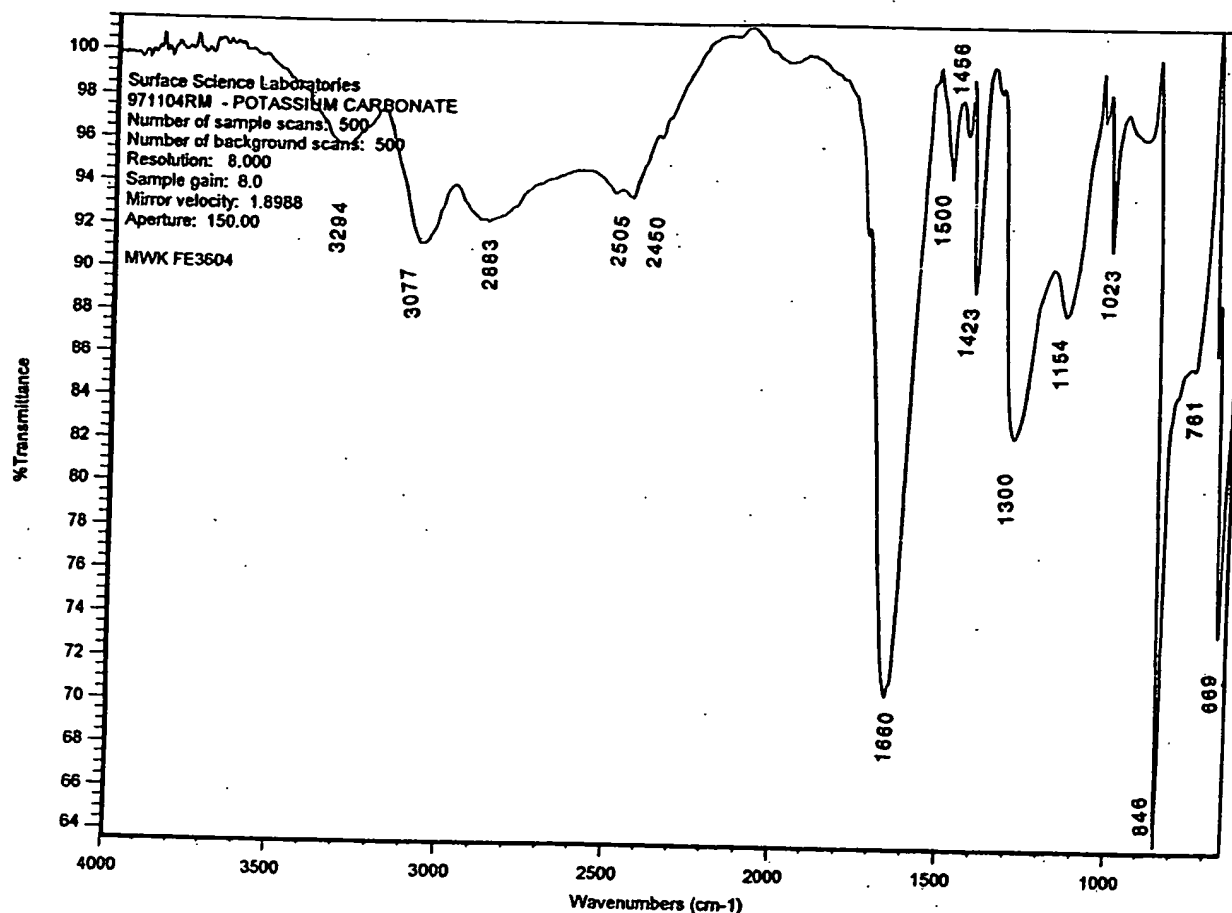
Fig. 23. The FTIR spectrum of polymeric material prepared by concentrating the K_2CO_3 electrolyte from the Thermacore electrolytic cell until a precipitate just formed (sample 2) from which the FTIR spectrum of the reference potassium carbonate was digitally subtracted.

potassium carbonate, but they are shifted $\sim$50 cm^{-1} to lower frequencies. The shifts are similar to those observed by replacing potassium (K_2CO_3) with rubidium (Rb_2CO_3), as demonstrated by comparing their infrared spectra.[11] The shifted peaks may be explained by a polymeric structure for the compound KH KHCO$_3$ identified by TOF-SIMS, XPS, and NMR.

III.E. Raman

The Raman spectrum of sample 3 appears in Fig. 25. In addition to the known peaks of KHCO$_3$ and a small peak assignable to K_2CO_3, unidentified peaks at 1685 and 835 cm^{-1} are present. The unidentified Raman peak at 1685 cm^{-1} is in the region of the N-H bonds. The FTIR spectrum of sample 2 also contains unidentified bands in the 1400- to 1600-cm^{-1} region. Samples 3 and 2 do not contain N-H bonds by XPS studies. The N 1s XPS peak of the former is at 393.6 eV, and the N 1s XPS peak of the latter is a very broad peak at $\sim$390 eV, whereas the N 1s XPS peak of compounds containing a N-H bond is

seen at $\sim$399 eV, and the lowest energy N 1s XPS peak for any known compound is $\sim$398 eV.

The 835-cm^{-1} peak of Raman sample 2 is in the region of the bridged and terminal metal-hydrogen bonds. The novel peaks without the identifying assignment correspond to and identify hydrino hydride compounds.

III.F. Nuclear Magnetic Resonance

The signal intensities of the ^{1}H MAS NMR spectrum of the K_2CO_3 reference were relatively low. It contained a water peak at 1.208 ppm, a peak at 5.604 ppm, and very broad weak peaks at 13.2 and 16.3 ppm. The ^{1}H MAS NMR spectrum of the KHCO$_3$ reference contained a large peak at 4.745 with a small shoulder at 5.150 ppm, a broad peak at 13.203 ppm, and small peak at 1.2 ppm.

The ^{1}H MAS NMR spectrum of electrolytic cell sample 2 is shown in Fig. 26. The peak assignments are given in Table VI. The reproducible peaks assigned to KH KHCO$_3$ in Table VI were not present in the controls except for the peak assigned to water at
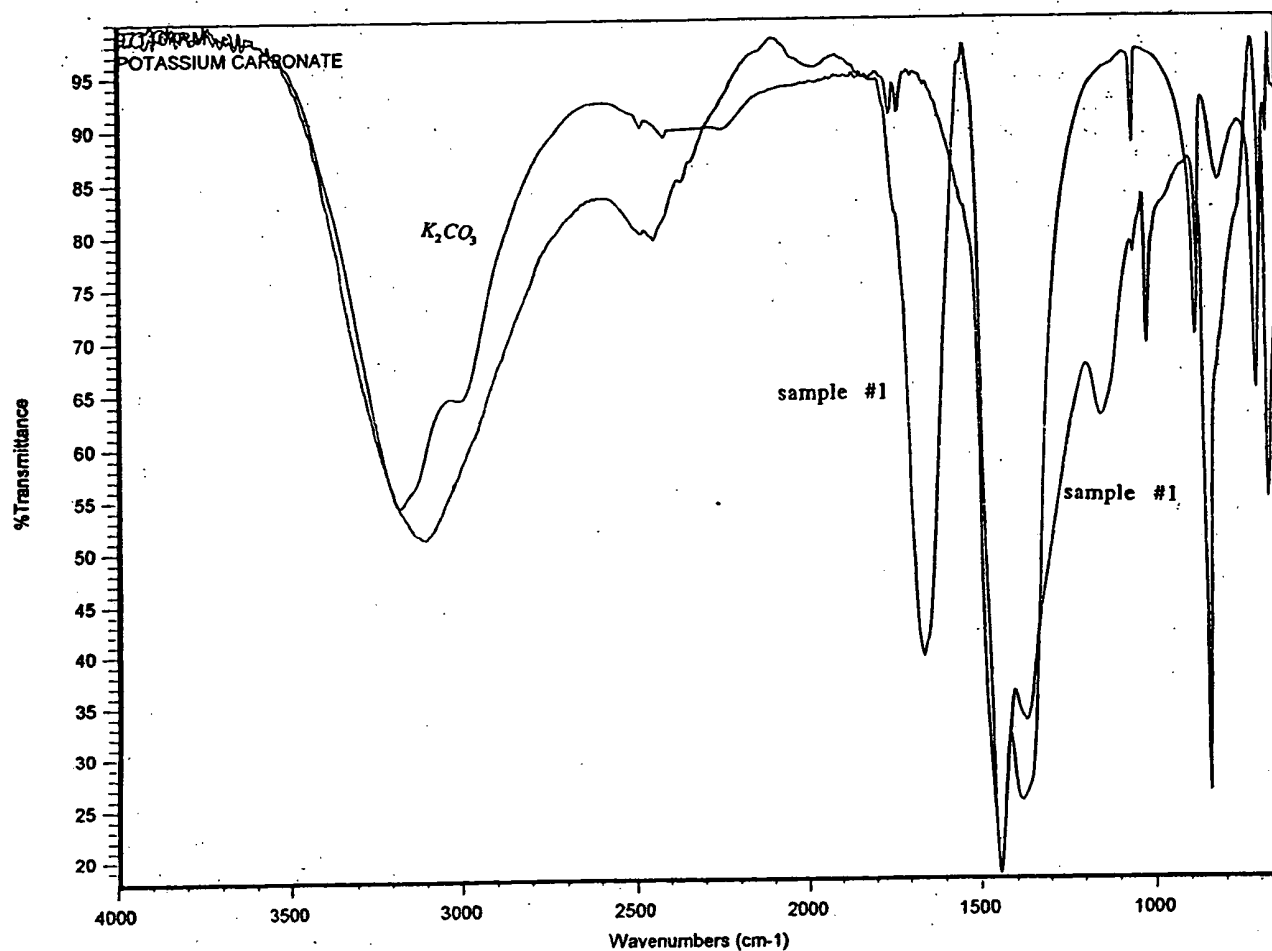
Fig. 24. The overlap FTIR spectrum of sample 2 and the FTIR spectrum of the reference potassium carbonate.
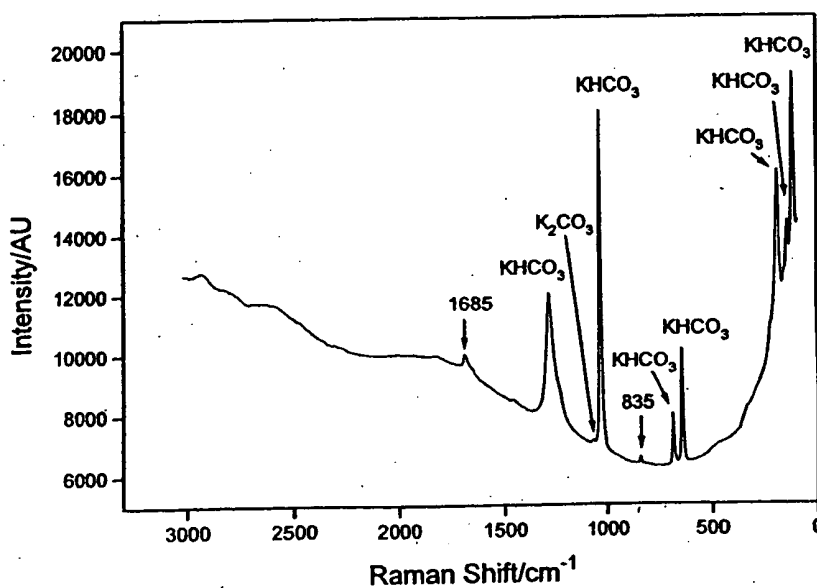

Fig. 25. The Raman spectrum of polymeric material prepared by concentrating the K_2CO_3 electrolyte from the Thermacore electrolytic cell until a precipitate just formed (sample 2).
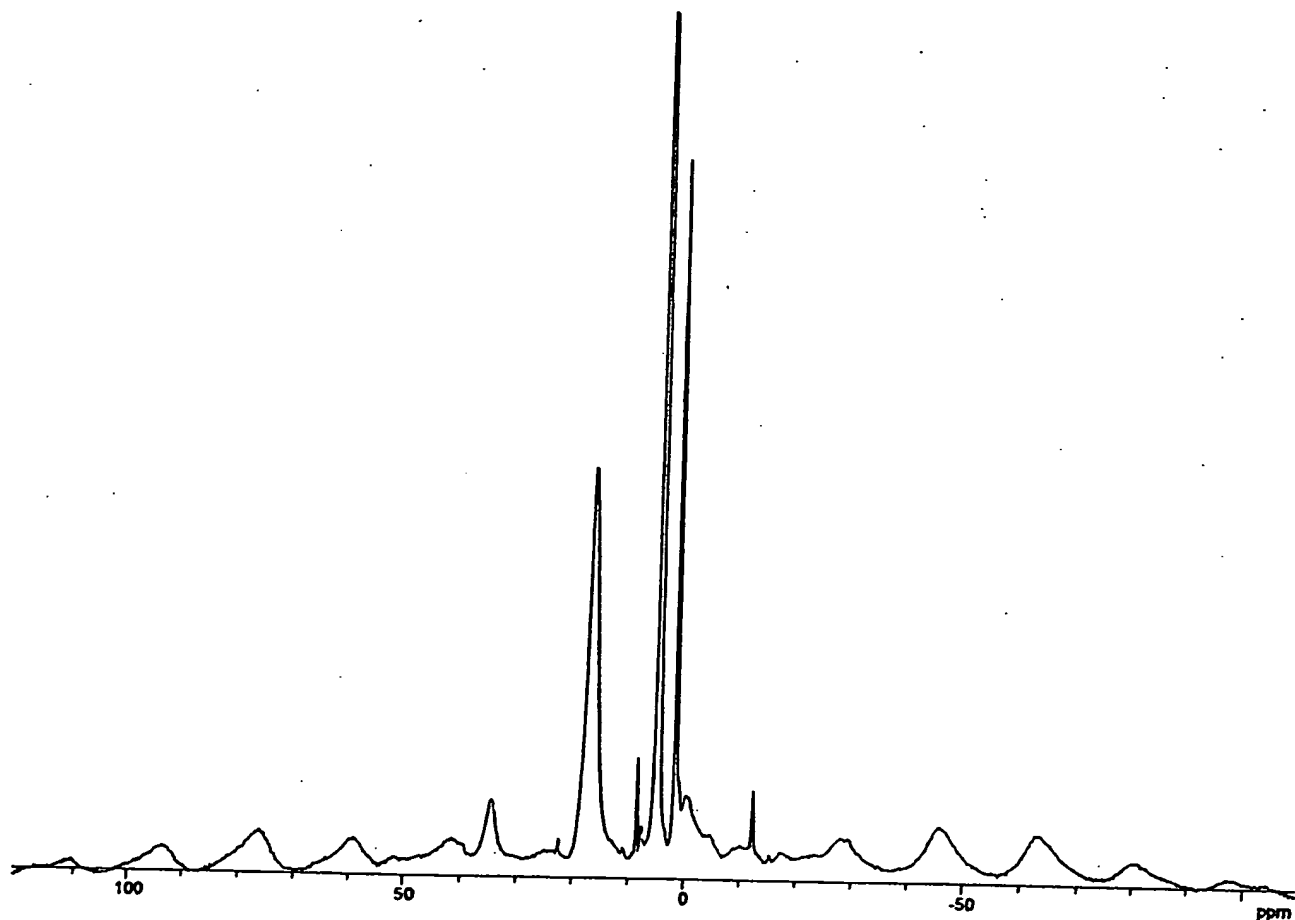
Fig. 26. The magic angle solid NMR spectrum of polymeric material prepared by concentrating the K_2CO_3 electrolyte from the Thermacore electrolytic cell until a precipitate just formed (sample 2).

+5.066 ppm. The novel peaks could not be assigned to hydrocarbons. Hydrocarbons were not present in the electrolytic cell sample 2 based on the TOF-SIMS spectrum and FTIR spectra. The novel peaks without identifying assignment are consistent with KH $KHCO_3$. The NMR peaks of the hydride ion of control potassium hydride were observed at 1.192 and 0.782 ppm relative to Tetra Methyl Silane (TMS). The upfield peaks of Fig. 26 are assigned to novel hydride ion (KH-) present in different environments. The downfield peaks are assigned to the proton of the potassium hydrogen carbonate species in different chemical environments ($-KHCO_3$).

IV. DISCUSSION

Alkali and alkaline earth hydrides react violently with water to release hydrogen gas, which subsequently ignites because of the exothermic reaction with water. Typically, metal hydrides decompose upon heating at a temperature well below the melting point of the parent

metal. These saline hydrides, so called because of their saltlike or ionic character, are the monohydrides of the alkali metals and the dihydrides of the alkaline-earth metals, with the exception of beryllium. BeH_2 appears to be a hydride with bridge-type bonding rather than an ionic hydride. Highly polymerized molecules held together by hydrogen-bridge bonding are exhibited by boron hydrides and aluminum hydride. Based on the known structures of these hydrides, the TOF-SIMS hydride clusters such as $K[KH\ KHCO_3]_n^+$, the XPS peaks observed at 22.8 and 38.8 eV, the upfield NMR peaks assigned to hydride ion, and the shifted FTIR peaks, the present novel hydride compound may be a polymer, $[KH\ KHCO_3]_n$, with a structural formula that is similar to boron and aluminum hydrides. The reported novel compound appeared polymeric in the concentrated electrolytic solution and in distilled water. Whereas potassium hydride reacts violently with water, $[KH\ KHCO_3]_n$ is extraordinarily stable in water.

As an example of the structures of this compound, the $K[KH\ KHCO_3]_n^+$ $m/z = (39 + 140n)$ series of fragment peaks is tentatively assigned to novel hydride
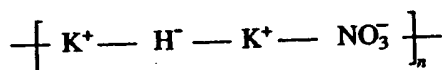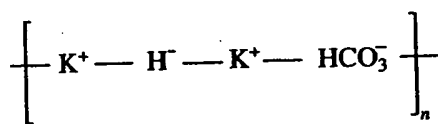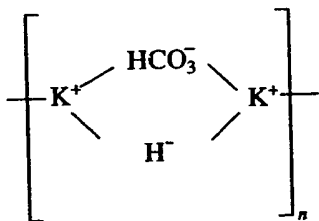
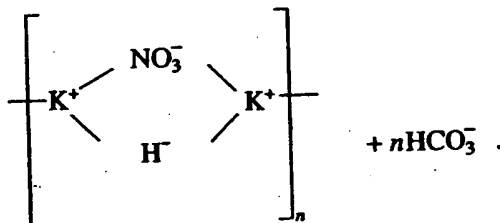TABLE VI

The NMR Peaks of Sample 2 with Their Assignments

Peak at Shift (ppm)	Assignment
+34.54	Side band of +17.163 peak
+22.27	Side band of +5.066 peak
+17.163	KH KHCO$_3$
+10.91	KH KHCO$_3$
+8.456	KH KHCO$_3$
+7.50	KH KHCO$_3$
+5.066	H$_2$O
+1.830	KH KHCO$_3$
−0.59	Side band of +17.163 peak
−12.05	KH KHCO$_3$[a]
−15.45	KH KHCO$_3$

[a]Small shoulder is observed on the −12.05 peak, which is the side band of the +5.066 peak.

bridged or linear potassium bicarbonate compounds having a general formula such as $[KHKHCO_3]_n$ $n = 1,2,3....$ General structural formulas may be

$$\left[\begin{array}{c} K^+ \diagup \overset{HCO_3^-}{\diagdown} K^+ \\ \diagdown \underset{H^-}{\diagup} \end{array}\right]_n$$

$$\left[\; K^+ — H^- — K^+ — HCO_3^- \;\right]_n \xrightarrow{\;NO_3^-\;}$$

$$\left[\; K^+ — H^- — K^+ — NO_3^- \;\right]_n$$

or

$$\left[\begin{array}{c} K^+ \diagup \overset{NO_3^-}{\diagdown} K^+ \\ \diagdown \underset{H^-}{\diagup} \end{array}\right]_n + nHCO_3^- .$$

and

$$\left[\; K^+ — H^- — K^+ — HCO_3^- \;\right]_n \cdot$$

Liquid chromatography/ESITOFMS studies are in progress to support the polymer assignment.

The observation of inorganic hydride fragments such as $K[KH\ KHCO_3]^+$ in the positive TOF-SIMS spectra of samples isolated from the electrolyte following acidification indicates the stability of the novel potassium hydride potassium bicarbonate compound.[1] The electrolyte was acidified with HNO_3 to pH = 2 and boiled to dryness to prepare samples to determine whether KH KHCO$_3$ was reactive under these conditions. Ordinarily, no K_2CO_3 would be present, and the sample would be converted to KNO_3. Crystals were isolated by dissolving the dried crystals in water, concentrating the solution, and allowing crystals to precipitate. TOF-SIMS was performed on these crystals. The positive spectrum contained elements of the series of inorganic hydride clusters $\{K[KH\ KHCO_3]_n^+\ m/z = (39 + 140n),\ K_2OH[KH\ KHCO_3]_n^+\ m/z = (95 + 140n),\ and\ K_3O[KH\ KHCO_3]_n^+\ m/z = (133 + 140n)\}$, which were observed in the positive TOF-SIMS spectrum of electrolytic cell sample 1 as discussed in Sec. III.A and given in Figs. 3 and 4 and Table I. The presence of bicarbonate carbon (C $1s \cong 289$ eV) was observed in the XPS of the sample from the HNO$_3$ acidified electrolyte. In addition, fragments of compounds formed by the displacement of hydrogen carbonate by nitrate were observed.[1] A general structural formula for the reaction may be
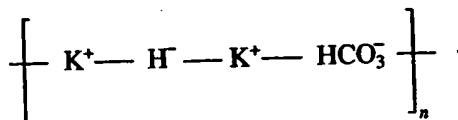
(10)

During acidification of the K_2CO_3 electrolyte, the pH repetitively increased from 3 to 9, at which time additional acid was added with a carbon dioxide release. The increase in pH (release of base by the titration reactant) was dependent on the temperature and concentration of the solution. A reaction consistent with this observation is the displacement reaction of NO_3^- for HCO_3^{2-}, as given by Eq. (10).

V. CONCLUSION

The TOF-SIMS, XPS, and NMR results confirm the identification of KH KHCO$_3$ with a new state of hydride ion. The chemical structure and properties of this compound having a hydride ion with a high binding energy as well as the observation of additional high binding energy hydride ions by XPS are indicative of a new field of hydride chemistry. Novel hydride ions may combine with other cations such as other alkali cations and alkaline earth, rare earth, and transition element cations. Thousands of novel compounds may be synthesized with extraordinary properties relative to the corresponding compounds having ordinary hydride ions if they exist. These novel compounds may have a breadth of applications. For example, according to the hydride binding energies observed as high as 70 eV by XPS, a high-voltage battery having projected specifications that surpass those of the internal combustion engine may be possible.

The TOF-SIMS, XPS, XRD, FTIR, Raman, and NMR results confirm the identification of hydrogen in new states: hydride ions of increased binding energy, inorganic hydrogen polymers, and hydrogen polymers. Work in progress demonstrates that bulk, pure compounds comprising new states of hydrogen may be formed by reaction of a gaseous catalyst with atomic hydrogen. In addition to TOF-SIMS, inorganic hydrogen compounds, alkali and alkaline earth hydrides, and polyhydrogen species were observed by ESITOFMS, solids-probe-magnetic-sector-mass spectroscopy, and solids-probe-quadrupole mass spectroscopy. Novel inorganic hydrogen compounds were also identified by liquid chromatography/mass spectroscopy. The chemical structures and properties of compounds comprising these new states of hydrogen are indicative of a new field of hydrogen chemistry.

Novel hydride and novel hydrogen chemistry also represents a new energy source. The exothermic reactions Eqs. (6), (7), (8), and (2), and the enthalpy of formation of KH KHCO$_3$ could explain the observation of excess enthalpy of 1.6×10^9 J that exceeded the total input enthalpy given by the product of the electrolysis voltage and current over time by a factor >8 reported previously.[2] Since the author's original publication of the possibility of producing atomic hydrogen energy states below the 13.6-eV level with the release of heat[12] followed by a report of lower energy molecular hydrogen,[2,13] other researchers have considered the possibility of sub-13.6-eV-state hydrogen.[14-17] The author's prediction and confirmation of novel hydride ions whereby the corresponding novel hydride compounds can be reproducibly made in bulk may lead to an explosion of development in this field.

ACKNOWLEDGMENTS

REFERENCES

1. R. MILLS, *The Grand Unified Theory of Classical Quantum Mechanics*, BlackLight Power (Jan. 1999).

2. R. MILLS, W. R. GOOD, and R. M. SHAUBACH, "Dihydrino Molecule Identification," *Fusion Technol.*, 25, 103 (1994).

3. M. G. JACOX and K. D. WATTS, "The Search for Excess Heat in the Mills Electrolytic Cell," Idaho National Engineering Laboratory (Jan. 7, 1993).

4. *Microsc. Microanal. Microstruct.*, 3, 1 (1992).

5. "PHI Trift II," TOF-SIMS Technical Brochure, Physical Electronics, Eden Prairie, Minnesota.

6. "Practical Surface Analysis," *Ion and Neutral Spectroscopy*, Vol. 2, 2nd ed., D. BRIGGS and M. P. SEAH, Eds., John Wiley & Sons, New York (1992).

7. *Handbook of X-Ray Photoelectron Spectroscopy*, C. D. WAGNER, W. M. RIGGS, L. E. DAVIS, J. F. MOULDER, and G. E. MULILENBERG, Eds., Physical Electronics, Eden Prairie, Minnesota (1997).

8. *CRC Handbook of Chemistry and Physics*, 58th ed., pp. B-143 and B-161, R. C. WEAST, Ed., CRC Press, Boca Raton, Florida (1977).

9. D. LIN-VIEN, N. B. COLTHUP, W. G. FATELEY, and J. G. GRASSELLIC, *The Handbook of Infrared and Raman Characteristic Frequencies of Organic Molecules*, Academic Press, New York (1991).

10. *Infrared Spectra of Inorganic Compounds*, R. A. NYQUIST and R. O. KAGEL, Eds., Academic Press, New York (1971).

11. M. H. BROOKER and J. B. BATES, *Spectrochim. Acta*, 30A, 2211 (1994).

12. R. L. MILLS and S. P. KNEIZYS, "Excess Heat Production by the Electrolysis of an Aqueous Potassium Carbonate Electrolyte and the Implications for Cold Fusion," *Fusion Technol.*, 20, 65 (1991).

13. R. MILLS and W. R. GOOD, "Fractional Quantum Energy Levels of Hydrogen," *Fusion Technol.*, 28, 1697 (1995).

14. J. P. VIGIER, "New Hydrogen Energies in Specially Structured Dense Media: Capillary Chemistry and Capillary Fusion," *Proc. 3rd Annual Conf. Cold Fusion*, Nagoya, Japan, October 21-25, 1992, p. 325, H. IKEGAMI, Ed., Universal Academy Press, Tokyo (1992).

15. J. P. VIGIER, "New Hydrogen (Deuterium) Bohr Orbits," *Proc. ICCF4*, Vol. 4, p. 7-1 (1994).

16. J. A. MALY and J. VÁVRA, "Electron Transitions on Deep Dirac Levels I," *Fusion Technol.*, 24, 307 (1993).

17. J. DUFOUR, J. FOOS, J. P. MILLOT, and X. DUFOUR, "Interaction of Palladium/Hydrogen and Palladium/Deuterium to Measure the Excess Energy per Atom for Each Isotope," *Fusion Technol.*, 31, 198 (1997).

Randell L. Mills (BA, chemistry, Franklin and Marshall College, 1982; MD, Harvard Medical School, 1986) is the founder of BlackLight Power, located in the Princeton, New Jersey area, which has developed a new hydrogen chemical process for generating thermal energy for heating, electrical power generation, and motive power. The products of the reaction may represent a vast class of new compositions of matter.